

Journal Pre-proof

Synthesis and Characterization of 1,2,4-Triazolo[1,5-*a*]pyrimidine-2-carboxamide-based Compounds Targeting the PA-PB1 Interface of Influenza A Virus Polymerase

Serena Massari, Chiara Bertagnin, Maria Chiara Pismataro, Anna Donnadio, Giulio Nannetti, Tommaso Felicetti, Stefano Di Bona, Maria Giulia Nizi, Leonardo Tensi, Giuseppe Manfroni, Maria Isabel Loza, Stefano Sabatini, Violetta Cecchetti, Jose Brea, Laura Goracci, Arianna Loregian, Oriana Tabarrini



PII: S0223-5234(20)30916-8

DOI: <https://doi.org/10.1016/j.ejmech.2020.112944>

Reference: EJMECH 112944

To appear in: *European Journal of Medicinal Chemistry*

Received Date: 13 September 2020

Revised Date: 13 October 2020

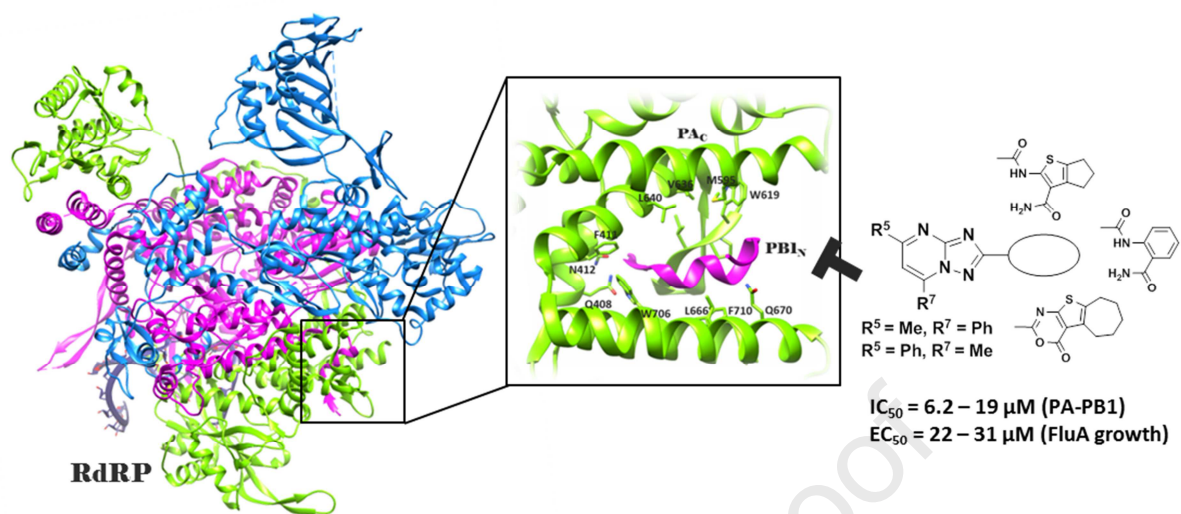
Accepted Date: 13 October 2020

Please cite this article as: S. Massari, C. Bertagnin, M.C. Pismataro, A. Donnadio, G. Nannetti, T. Felicetti, S. Di Bona, M.G. Nizi, L. Tensi, G. Manfroni, M.I. Loza, S. Sabatini, V. Cecchetti, J. Brea, L. Goracci, A. Loregian, O. Tabarrini, Synthesis and Characterization of 1,2,4-Triazolo[1,5-*a*]pyrimidine-2-carboxamide-based Compounds Targeting the PA-PB1 Interface of Influenza A Virus Polymerase, *European Journal of Medicinal Chemistry*, <https://doi.org/10.1016/j.ejmech.2020.112944>.

This is a PDF file of an article that has undergone enhancements after acceptance, such as the addition of a cover page and metadata, and formatting for readability, but it is not yet the definitive version of record. This version will undergo additional copyediting, typesetting and review before it is published in its final form, but we are providing this version to give early visibility of the article. Please note that, during the production process, errors may be discovered which could affect the content, and all legal disclaimers that apply to the journal pertain.

© 2020 Elsevier Masson SAS. All rights reserved.

Graphical Abstract



Synthesis and Characterization of 1,2,4-Triazolo[1,5-*a*]pyrimidine-2-carboxamide-based Compounds Targeting the PA-PB1 Interface of Influenza A Virus Polymerase

Serena Massari,^{a,*} Chiara Bertagnin,^b Maria Chiara Pismataro,^a Anna Donnadio,^a Giulio Nannetti,^b Tommaso Felicetti,^a Stefano Di Bona,^c Maria Giulia Nizi,^a Leonardo Tensi,^c Giuseppe Manfroni,^a Maria Isabel Loza,^d Stefano Sabatini,^a Violetta Cecchetti,^a Jose Brea,^d Laura Goracci,^c Arianna Loregian,^{b,#} Oriana Tabarrini.^{a,#}

^a Department of Pharmaceutical Sciences, University of Perugia, 06123 Perugia, Italy

^b Department of Molecular Medicine, University of Padua, 35121 Padua, Italy

^c Department of Chemistry, Biology and Biotechnology, University of Perugia, 06123 Perugia, Italy

^d CIMUS Research Center, University of Santiago de Compostela, 15782, Santiago de Compostela, Spain

*Corresponding authors: Serena Massari, Department of Pharmaceutical Sciences, University of Perugia, 06123 Perugia, Italy; Tel: +39 075-5855134, Fax: +39 075-5855115, *E-mail*: serena.massari@unipg.it

Co-last authors

Abstract

Influenza viruses (Flu) are responsible for seasonal epidemics causing high rates of morbidity, which can dramatically increase during severe pandemic outbreaks. Antiviral drugs are an indispensable weapon to treat infected people and reduce the impact on human health, nevertheless anti-Flu armamentarium still remains inadequate.

In search for new anti-Flu drugs, our group has focused on viral RNA-dependent RNA polymerase (RdRP) developing disruptors of PA-PB1 subunits interface with the best compounds characterized by cycloheptathiophene-3-carboxamide and 1,2,4-triazolo[1,5-*a*]pyrimidine-2-carboxamide scaffolds. By merging these moieties, two very interesting hybrid compounds were recently identified, starting from which, in this paper, a series of analogues were designed and synthesized. In particular, a thorough exploration of the cycloheptathiophene-3-carboxamide moiety led to acquire important SAR insight and identify new active compounds showing both the ability to inhibit PA-PB1 interaction and viral replication in the micromolar range and at non-toxic concentrations. For few compounds, the ability to efficiently inhibit PA-PB1 subunits interaction did not translate into anti-Flu activity. Chemical/physical properties were investigated for a couple of compounds suggesting that the low solubility of compound **14**, due to a strong crystal lattice, may have impaired its antiviral activity. Finally, computational studies performed on compound **23**, in which the phenyl ring suitably replaced the cycloheptathiophene, suggested that, in addition to hydrophobic interactions, H-bonds enhanced its binding within the PA_C cavity.

Keywords: Influenza virus, PA-PB1 heterodimerization, RNA-dependent RNA polymerase, protein-protein interaction.

1. Introduction

Influenza (Flu) viruses are responsible for seasonal epidemics resulting in about 3 to 5 million cases of severe respiratory illness and 290,000 to 650,000 deaths each year all over the world [1]. Moreover, they are also able to generate pandemic outbreaks that occur when new highly virulent FluA subtypes generated by antigenic shift are transmitted from animals to humans and sustainably spread among people.

In 1918, humanity experienced the “Spanish Flu” caused by FluA(H1N1) [2], an influenza pandemic that intensively and speedily struck world population infecting about 500 million people and killing from 20 to 40 million people globally [3]. Other two pandemics occurred in 20th century: the “Asian Flu” caused by Flu A(H2N2) virus [4], which started in China in 1957 and spread globally causing about one to four million deaths, and the “1968 Flu pandemic” caused by Flu A(H3N2) virus, which started in Hong Kong and spread to the United States causing one million deaths. In 2003, the avian Flu A(H5N1) re-emerged passing the species barrier but fortunately not spreading sustainably from person to person, while, in 2009, the “swine Flu” A(H1N1) virus was responsible for the first pandemic of the 21st century [5]; it started in Mexico and spread rapidly around the world causing from 150,000 to 600,000 deaths [6]. To date, the avian Flu A(H5N1) and Flu A(H7N9) are of particular concern to public health due to their potential to cause an influenza pandemic [7].

Previous pandemic events from Flu viruses highlighted that a vaccine is an essential mean to rapidly prevent the spread of infection, but, in the absence of a vaccine, antiviral drugs could be a valid weapon to treat infected people and reduce the impact on human health. Unfortunately, a universal anti-Flu vaccine does not exist yet, so in case of a pandemic event, a new specific vaccine should be developed on the basis of the emerging strain.

Regarding the anti-flu treatment, until recently, the only approved anti-Flu drugs were the NA inhibitors oseltamivir and zanamivir (laninamivir octanoate and peravimivir were approved only in some Asian countries), and adamantanes targeting the M2 ion channels protein, although the latter

are no longer recommended due to the emergence of widespread resistance [8]. This limited therapeutic armamentarium was recently enriched by a new class of anti-Flu drugs involved in the inhibition of the RNA-dependent RNA polymerase (RdRP) [9–12]. In particular, the nucleoside analog favipiravir was approved in 2014 in Japan for stockpiling against Flu pandemics [13]; to date, the safety and efficacy of favipiravir are also being evaluated in seven clinical trials against COVID-19. In 2018, the endonuclease inhibitor baloxavir marboxil was approved in both Japan and the United States [14]; moreover, the cap-binding inhibitor pimodivir is currently in late phase clinical trials [15].

The RdRP is thus emerging as an important drug-target [16–18]. It is a heterotrimer composed by the polymerase basic protein 1 (PB1), polymerase basic protein 2 (PB2), and polymerase acidic protein (PA, P3 in FluC) subunits. The three RdRP subunits are connected in head-to-tail fashion by extensive interactions that occur between the PB1_N and PA_C termini and the PB1_C and PB2_N termini. In the context of the viral ribonucleoprotein complex (vRNP), the RdRP plays a key role in the viral life cycle performing both the transcription and replication of viral genome [19,20].

The publication of crystal structures of PA_C-PB1_N interface (pdb codes: 3CM8 [21] and 2ZNL [22]) prompted the search for small-molecule inhibitors of this protein-protein interaction (PPI) able to interfere with RdRP functions [23–25]. We have been pioneers in this research field, identifying several compounds characterized by different chemotypes. In particular, with the exception of a compound AL18 that was found serendipitously [26], all the other PA-PB1 inhibitors have been identified by an initial structure-based drug design [27,28] followed by hit-to-lead optimization campaigns, such as cycloheptathiophene-3-carboxamide (cHTC) [29–31], 1,2,4-triazolo[1,5-*a*]pyrimidine (TZP) [32], pyrazolo[1,5-*a*]pyrimidine [33] and 3-cyano-4,6-diphenylpyridine [34] derivatives. During the optimization of cHTC derivative **1** [27] and TZP derivative **2** [27] (Figure 1), hybrid compounds **3** and **4** (Figure 1) were prepared by joining the cHTC and the TZP moieties, exhibiting very interesting activities [32]. In particular, compound **3**, with an IC₅₀ = 1.1 μM, emerged as one of the most potent among the small-molecule PA-PB1 inhibitors developed so far.

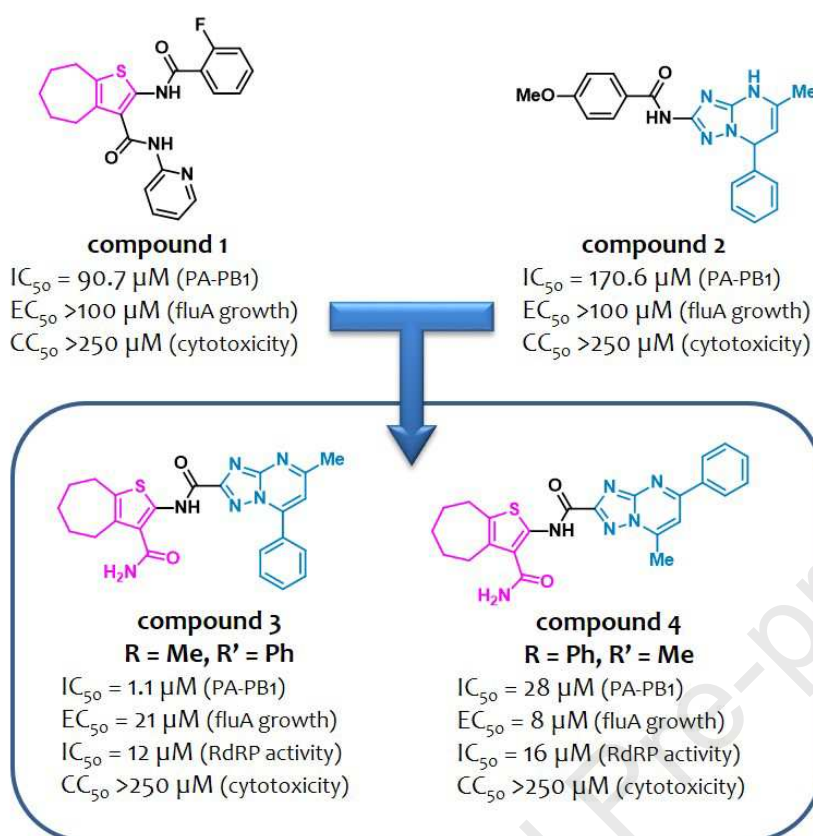


Figure 1. Structures and biological activities of compounds **1-4** previously reported [27,32].

Accordingly, it affected PA-PB1 binding in the cell cytoplasm and blocked the intranuclear translocation of PA, which requires the formation of the PA-PB1 complex. Compound **3** also showed good anti-polymerase activity ($IC_{50} = 12 \mu\text{M}$ in minireplicon assay) and broad anti-FluA and -FluB activity (EC_{50} s ranging from 7 to 25 μM , in MDCK cells) without showing any cytotoxicity up to concentrations of 250 μM . Compound **4** exhibited slightly better antiviral activity (EC_{50} values ranging from 5 to 14 μM against FluA and FluB strains), even if it was endowed with lower ability to inhibit the PA-PB1 interaction ($IC_{50} = 28 \mu\text{M}$) [32].

Computational studies performed on the positional isomers **3** and **4** within the PA_C cavity suggested that the molecules have a different orientation and extents of hydrophobic and H-bond interactions within the cavity [32]. Thus, while the elongated shape of **4** allows it to recognize all the three hydrophobic regions described by Liu and Yao [35] within the PB1 binding site, compound **3** is

shifted toward the opposite side of the cavity and matches only the first hydrophobic region, generated by W706. Nevertheless, compound **3** establishes a very favorable H-bond between its C-2 amidic carbonyl group and the Q408 residue, which could be the reason for its efficient inhibition of PA-PB1 heterodimerization.

In the present study, additional hybrid compounds were synthesized as analogues of compound **3** (compounds **5-18**, Figure 2) and compound **4** (compounds **19-26**, Figure 2). By mainly focusing on the cHTC core, various structural modifications were undertaken investigating the cycloheptane, the thiophene and the 2-carboxamide moieties. From the antiviral activity, SAR insights were obtained with the main indication entailing the favorable replacement of the cHTC core by a simpler 2-carbamoylphenyl moiety. In depth studies were pursued to determine the ability of the compounds to interfere with RdRP functions, their metabolic stability as well as to predict their binding mode within the PA_C cavity. Further studies were also performed on a couple of regioisomers to investigate the different behavior in inhibiting PA-PB1 interaction and viral growth.

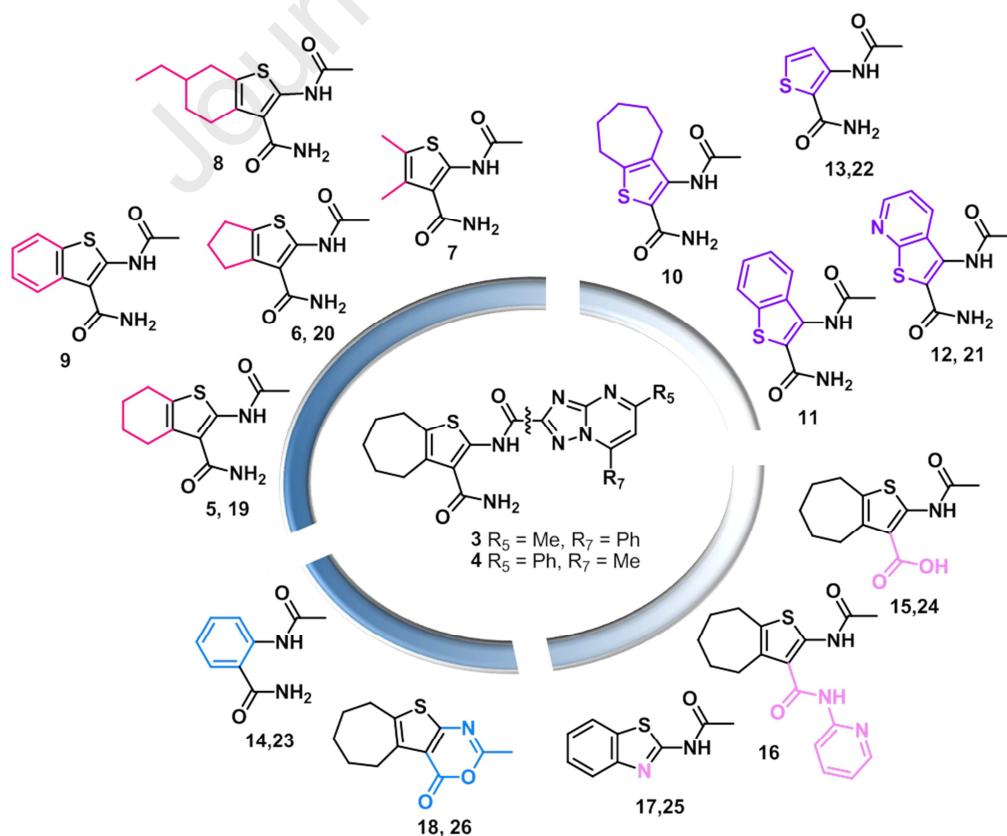
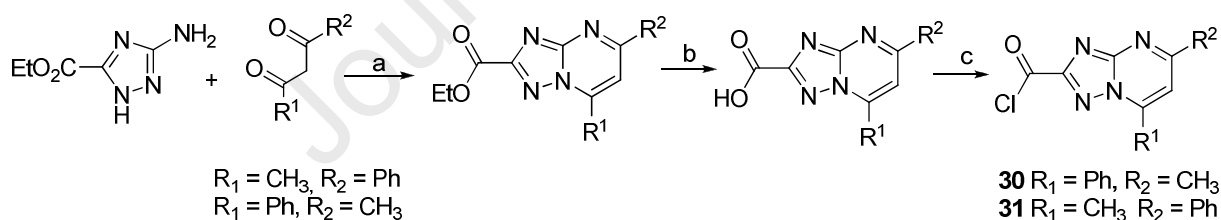


Figure 2. Structure of the compounds synthesized in this study. Compounds **5-18** are analogues of compound **3** and compounds **19-26** are analogues of compound **4**.

2. Results and Discussion

2.1. Chemistry

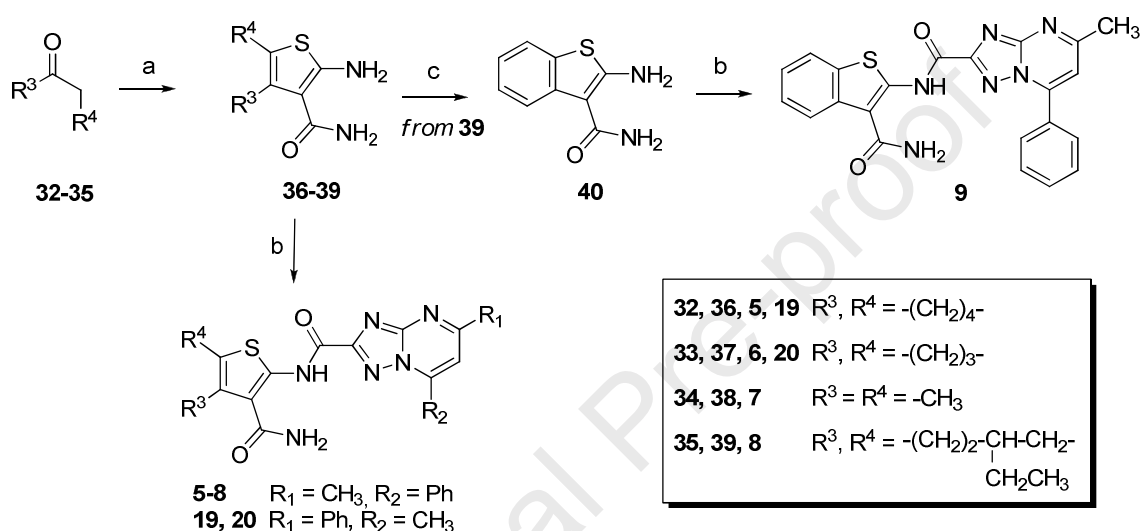
The synthesis of all the target compounds **5-13**, **15-22** and **24-29** was accomplished, as reported in Schemes 2-8, by coupling reaction of the appropriate reagent with 5-methyl-7-phenyl-[1,2,4]triazolo[1,5-*a*]pyrimidine-2-carbonyl chloride **30** [32] or 7-methyl-5-phenyl-[1,2,4]triazolo[1,5-*a*]pyrimidine-2-carbonyl chloride **31** [32]. As shown in Scheme 1, derivatives **30** and **31** were obtained by chlorination of the corresponding carboxylic acids [32], which were in turn prepared by cyclocondensation of ethyl 5-amino-1,2,4-triazole-3-carboxylate [36] and 1-phenylbutane-1,3-dione in acetic acid at reflux furnishing ethyl 5-methyl-7-phenyl-[1,2,4]triazolo[1,5-*a*]pyrimidine-2-carboxylate [37] and ethyl 7-methyl-5-phenyl-[1,2,4]triazolo[1,5-*a*]pyrimidine-2-carboxylate [37], followed by basic hydrolysis.



Scheme 1. Synthetic route of the intermediates **30** and **31**. Reagents and conditions: (a) glacial acetic acid, reflux; (b) NaOH, MeOH, reflux; (c) oxalyl chloride, CH_2Cl_2 , DMF, room temperature (r.t.).

The synthesis of tetrahydrobenzothiophene- (**5** and **19**), cyclopentathiophene- (**6** and **20**), 4,5-dimethylthiophene- (**7**), 6-ethyltetrahydrobenzothieno- (**8**), and benzothiophene- (**9**) 3-carboxamide derivatives entailed the preparation of reagent **36** [38], **37** [38], **38** [39], **39** [40], and **40** [41], respectively (Scheme 2). In particular, compounds **36-39** were obtained by applying the one-pot Gewald reaction entailing the reaction of alkyl ketones **32-35** with cyanoacetamide in the presence

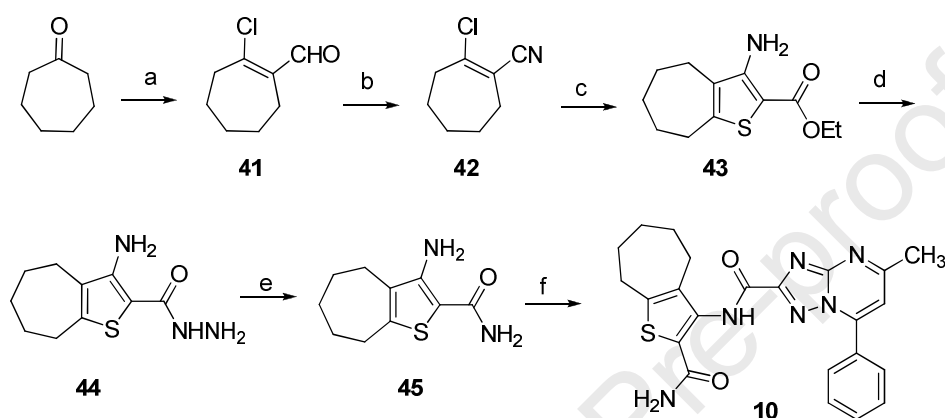
of sulphur and *N,N*-diethylamine or morpholine in EtOH. Then, by using conditions different from those reported in literature [41], compound **40** was obtained by oxidization of **39** by using *p*-chloranil in 1,4-dioxane. Coupling reaction of intermediates **36-39** with **30** and reagents **36** and **37** with **31** in CH₂Cl₂ in the presence of *N,N*-diisopropylethylamine (DIPEA) provided the target compounds **5-8**, **19** and **20**.



Scheme 2. Synthetic route of the target compounds **5-8**, **19** and **20**. Reagents and conditions: (a) sulphur, *N,N*-diethylamine, EtOH, rt or sulphur, morpholine, EtOH, reflux; (b) compound **30** or **31**, CH₂Cl₂, DIPEA, rt; (c) *p*-chloranil, 1,4-dioxane, 90 °C.

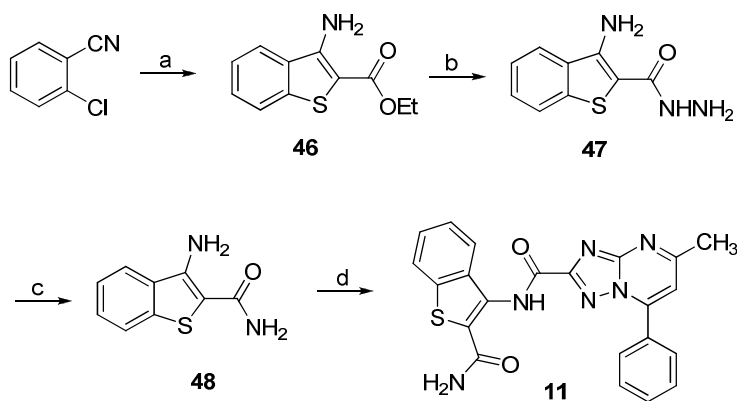
The synthesis of cHTC derivative **10** entailed the preparation of key intermediate **45**, as reported in Scheme 3. The preparation of thiophene-2-carboxamide derivatives was reported in literature by straight reaction of 2-chloro-cyanoderivatives with 2-mercaptoacetamide [42]. However, difficulties in the preparation of the latter as well as its commercial availability led us to undertake a different synthetic route entiling the preparation of ethyl carboxylate intermediate **43** and its successive transformation into carboxamide derivative **45**. In particular, cycloheptanone was reacted with DMF and POCl₃ to give intermediate **41** [43] that was used for the preparation of compound **42** [44] by reaction with hydroxylamine hydrochloride in *N*-methyl-2-pyrrolidinone (NMP). Intermediate

42 was then reacted with ethyl thioglycolate in presence of K_2CO_3 in a MeOH/THF mixture, to give compound **43** [45]. In order to convert the ethyl carboxylate moiety of compound **43** into a carboxamide group, it was reacted with hydrazine hydrate at 80 °C to give carbohydrazide derivative **44**, which was then treated with Ni-Raney in DMF at 90 °C providing compound **45**. Coupling reaction of **45** with **30** furnished the target derivative **10**.

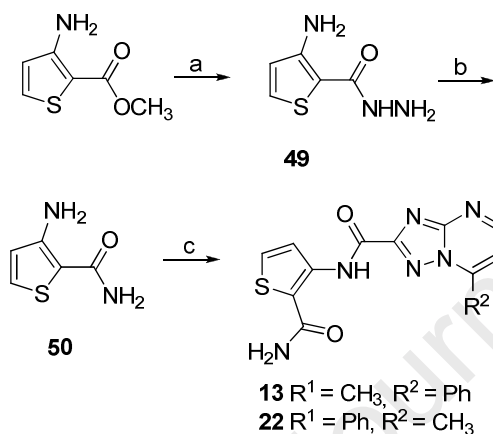


Scheme 3. Synthetic route of the target compound **10**. Reagents and conditions: (a) DMF, $POCl_3$, from 0 °C to r.t.; (b) NMP, NH_2OH hydrochloride, 115 °C; (c) K_2CO_3 , MeOH/THF (5:1), ethyl thioglycolate, reflux; (d) NH_2NH_2 hydrate, 80 °C; (e) Ni-Raney, DMF, 90 °C; (f) compound **30**, CH_2Cl_2 , DIPEA, rt.

Through an analogous procedure, benzothiophene-2-carboxamide derivative **11** and thiophene-2-carboxamide derivatives **13** and **22** were prepared as reported in Schemes 4 and 5, respectively. Thus, ethyl carboxylate derivative **46** [46], prepared by reacting 2-chlorobenzonitrile and ethyl thioglycolate in presence of KOH in DMF, and methyl 3-aminothiophene-2-carboxylate were reacted with hydrazine hydrate providing carbohydrazide derivatives **47** [47] and **49** [47], which were in turn treated with Ni-Raney to give carboxamide derivatives **48** [48] and **50** [49], respectively. Coupling reaction of **48** with **30** and **50** with **30** and **31** provided derivatives **11**, **13** and **22**, respectively.

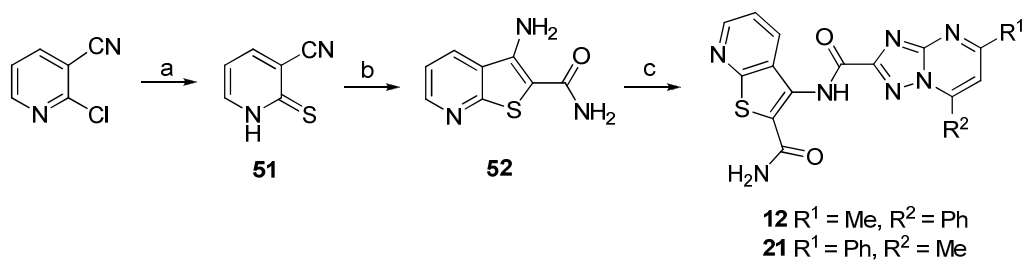


Scheme 4. Synthetic route of the target compound **11**. Reagents and conditions: (a) ethyl thioglycolate, DMF, KOH, from 0 °C to 80 °C; (b) NH_2NH_2 hydrate, 80 °C; (c) Ni-Raney, DMF, 90 °C; (d) compound **30**, CH_2Cl_2 , DIPEA, rt.



Scheme 5. Synthetic route of the target compounds **13** and **22**. Reagents and conditions: (a) NH_2NH_2 hydrate, 80 °C; (b) Ni-Raney, DMF, 90 °C; (c) compound **30** or **31**, CH_2Cl_2 , DIPEA, rt.

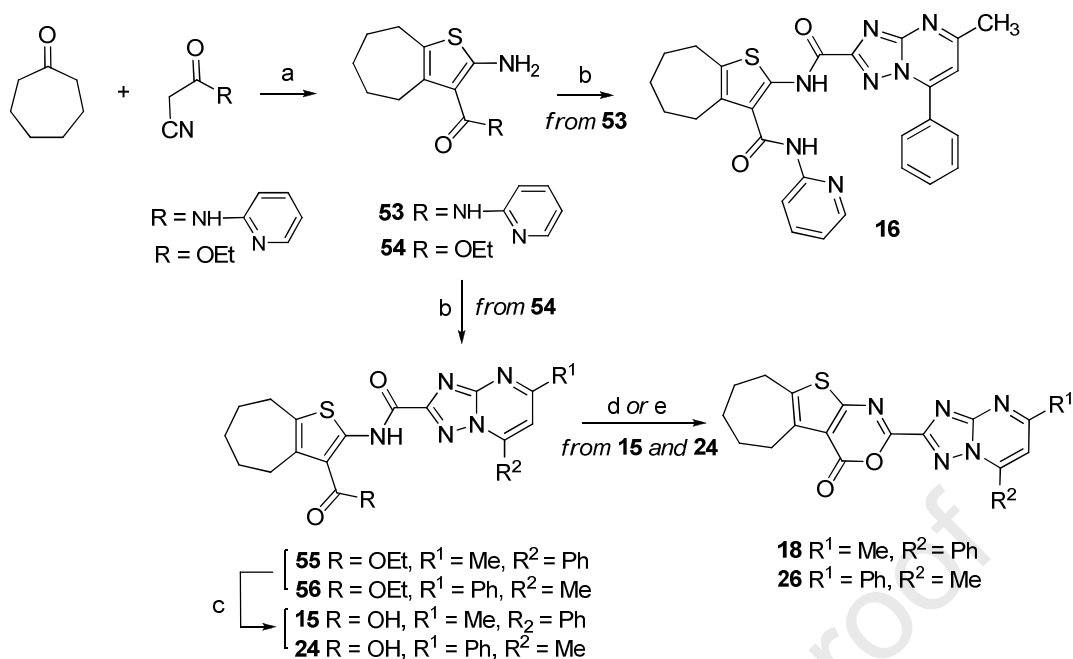
Thienopyridine-2-carboxamide derivatives **12** and **21** were prepared, as reported in Scheme 6, by coupling reaction of **30** and **31**, respectively, with carboxamide derivative **52** [50], which was obtained by reaction of 2-chloroniconitrile and thiourea in EtOH at reflux to give intermediate **51**, followed by reaction with 2-bromoacetamide in DMF in the presence of DIPEA.



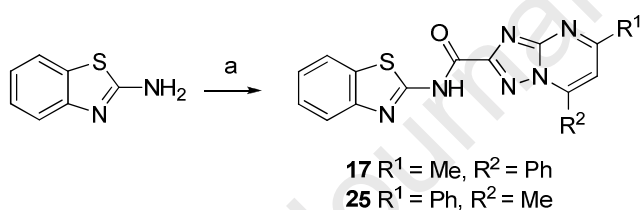
Scheme 6. Synthetic route of the target compound **12** and **21**. Reagents and conditions: (a) thiourea, EtOH, reflux; (b) 2-bromoacetamide, DIPEA, DMF, rt; (c) compound **30** or **31**, CH₂Cl₂, DIPEA, rt.

A one-pot Gewald reaction was initially applied for the synthesis of derivatives **16** bearing a C-3 pyridin-2-yl-carbamoyl moiety, **15** and **24** characterized by a C-3 carboxylic acid, and cycloheptathienooxazinones **18** and **26** (Scheme 7). Thus, cycloheptanone was reacted with 2-cyano-*N*-pyridin-2-ylacetamide [51] and ethyl 2-cyanoacetate, providing intermediates **53** [29] and **54** [52], respectively. Reagent **53** was then coupled with **30** to give target compound **16**, while reagent **54** was reacted with **30** and **31** yielding ethyl ester intermediates **55** and **56**, respectively. Hydrolysis under basic conditions of **55** and **56** provided acid derivatives **15** and **24**, which were in turn cyclized to give tricyclic derivatives **18** and **26**. Cyclization of acid **15** was performed in acetic anhydride at 100 °C providing **18** in very low yield (19%). As a consequence, cyclization of **24** was performed through an alternative procedure entailing the use of EDC, DIPEA, and 1-hydroxybenzotriazole in CH₂Cl₂, which permitted to obtain derivative **26** in 52% yield.

Finally, benzothiazole derivatives **17** and **25** were synthesized as reported in Scheme 8, by coupling reaction of 2-aminobenzothiazole with **30** and **31**, respectively.



Scheme 7. Synthetic route of the target compounds **15**, **24**, **18** and **26**. Reagents and conditions: (a) sulphur, *N,N*-diethylamine, EtOH, rt; (b) compound **30** or **31**, CH_2Cl_2 , DIPEA, rt; (c) LiOH, $\text{H}_2\text{O}/\text{THF}$ (1:1), $50\text{ }^\circ\text{C}$; (d) Ac_2O , $100\text{ }^\circ\text{C}$; (e) DIPEA, EDC, HOBT, CH_2Cl_2 , from $0\text{ }^\circ\text{C}$ to rt.



Scheme 8. Synthetic route of the target compounds **17** and **25**. Reagents and conditions: (a) compound **30** or **31**, CH_2Cl_2 , DIPEA, rt.

2.2. Inhibition of PA-PB1 heterodimerization and evaluation of anti-Flu activity

The study started from hit compound **3**, considering its better ability to interfere with PA-PB1 interaction. In particular, compounds **5-18** (Table 1) were synthesized by structurally modifying the cycloheptane, the thiophene, and the 2-carboxamide moieties of compound **3**, while keeping the 5-methyl-7-phenyl-[1,2,4]triazolo[1,5-*a*]pyrimidine-2-carboxamide portion.

All the compounds were evaluated for their ability to inhibit the PA-PB1 subunits interaction in an ELISA-based assay, including the Tat-PB1₁₋₁₅ peptide as a positive control, and for the antiviral

activity in FluA virus-infected MDCK cells by plaque reduction assays (PRA) with the A/PR/8/34 (PR8) strain, using ribavirin (RBV), a known inhibitor of RNA viruses polymerase, as a positive control. To exclude that the observed antiviral activities could be due to toxic effects in the target cells, all the compounds were tested in parallel by MTT assays in MDCK cells.

Regarding the modifications made on the cycloheptane ring, size reduction from cycloheptathiophene to tetrahydrobenzothiophene (compound **5**) and cyclopentathiophene (compound **6**) provided compounds showing a comparable anti-Flu activity ($EC_{50} = 32$ and $22 \mu\text{M}$, respectively, vs $21 \mu\text{M}$ of **3**) but a slightly decreased ability to inhibit PA-PB1 interaction ($IC_{50} = 15$ and $6.2 \mu\text{M}$, respectively) with respect to **3** ($IC_{50} = 1.1 \mu\text{M}$). On the other hand, the deletion of the cycloheptane ring gave 4,5-dimethylthiophene **7** devoid of both the activities. The alkylation and aromatization of the tetrahydrobenzene of compound **5** were explored in 6-ethyl-tetrahydrobenzothiophene **8** and benzothiophene **9**, respectively, which were both endowed with anti-Flu activity ($EC_{50} = 15$ and $49 \mu\text{M}$, respectively) but devoid of the ability to disrupt PA-PB1 interaction. Of note, derivative **8** emerged as the most active anti-Flu compound herein reported, even more than hit compound **3**. These results suggested that the presence of a cycloalkyl moiety fused to the thiophene ring is important to obtain anti-Flu activity, although its aromatization is still tolerated but detrimental for anti-PA-PB1 activity.

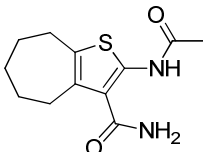
Then, a set of four derivatives was synthesized in which the thiophene-based core was linked to the TZP moiety by the C-3 position. The thienopyridine derivative **12** was the most potent PA-PB1 inhibitor among the compounds herein reported (IC_{50} of $3.3 \mu\text{M}$), but at the expense of the antiviral activity ($EC_{50} > 100 \mu\text{M}$), while derivative **13** exhibited a balanced biological profile (IC_{50} of $31 \mu\text{M}$ and EC_{50} of $43 \mu\text{M}$). These results indicated that, in this series of compounds, the lack of a cycloalkyl ring fused to the thiophene does not impair the activity.

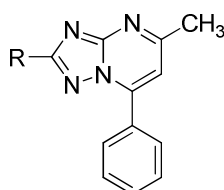
No anti-PA-PB1 activity was shown by cycloheptathiophene compound **10** and benzothiophene compound **11**, the strict analogs of compounds **3** and **9**, respectively, although the latter showed anti-Flu activity ($EC_{50} = 22 \mu\text{M}$) comparable to that of hit compound **3** ($EC_{50} = 21 \mu\text{M}$). Of note,

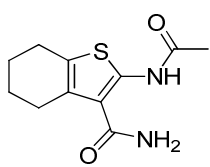
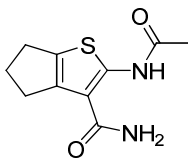
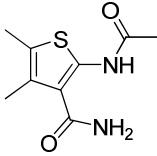
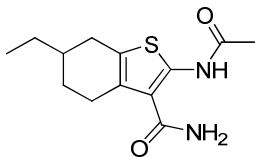
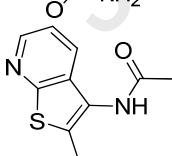
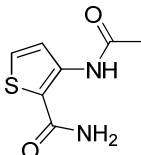
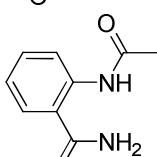
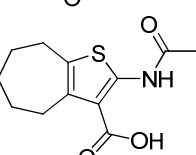
the whole cHTC core can be replaced by a simpler benzene ring to achieve anti-PA-PB1 activity, as shown by the 2-carbamoylphenyl derivative **14** [53], characterized by a good IC_{50} of 11 μM but devoid of anti-Flu activity. Finally, in order to explore the role of the C-3 carboxamide moiety, it was replaced by a bioisosteric carboxylic group or by an *N*-(2-pyridyl)-carboxamide moiety, which also characterized hit compound **1**, as in derivatives **15** and **16**, respectively. Moreover, a benzothiazole replaced the cycloheptathiophene ring in derivative **17**, while the two amide linkages at the C-2 and C-3 positions of the cycloheptathiophene were constrained into a 1,3-oxazinone ring in the tricyclic derivative **18**. The four compounds showed a comparable anti-PA-PB1 activity, with IC_{50} s ranging from 19 to 23 μM , and compounds **15** and **16** also shared a similar anti-Flu activity (EC_{50} = 50 and 48 μM , respectively). The benzothiazole ring (compound **17**) was not suitable for achieving anti-Flu activity, while the cycloheptathienooxazinone derivative **18** was the most active in inhibiting the viral growth with an EC_{50} of 26 μM .

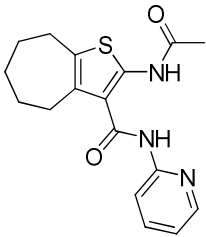
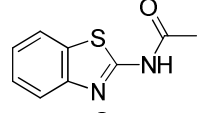
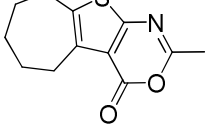
All the compounds were non-toxic up to 250 μM concentration, with the exception of derivatives **10** and **18**, which, however, showed a mild cytotoxic effect (CC_{50} = 90 and 101 μM , respectively).

Table 1. Structure and Biological Activity of Compound **3** Analogues.

Compd	R	ELISA PA-PB1 Interaction Assay IC_{50} , μM^a	PRA in MDCK cells EC_{50} , μM^b	Cytotoxicity in MDCK cells CC_{50} , μM^c
3		1.1 \pm 0.3	21 \pm 4	>250



5		15 ± 3	32 ± 8	>250
6		6.2 ± 0.3	22 ± 7	>250
7		>200	>50	>250
8		>200	15 ± 2	>250
9		>200	49 ± 1	>250
10		>200	>50	90 ± 7
11		>200	22 ± 4	>250
12		3.3 ± 0.7	>100	>250
13		31 ± 5	43 ± 2	250
14		11 ± 3	>100	>250
15		19 ± 1	50 ± 3	>250

16		23 ± 2	48 ± 2	>250
17		21 ± 1	>50	>250
18		19 ± 1	26 ± 1	101 ± 2
RBV			10 ± 2	>250
Tat-PB1₁₋₁₅ peptide		35 ± 4	41 ± 5	>100

^a Activity of the compounds in ELISA PA-PB1 interaction assays. The IC₅₀ value represents the compound concentration that reduces by 50% the interaction between PA and PB1. ^b Activity of the compounds in plaque reduction assays with the Flu A A/PR/8/34 strain. The EC₅₀ value represents the compound concentration that inhibits 50% of plaque formation. ^c Cytotoxicity of the compounds in MTT assays. The CC₅₀ value represents the compound concentration that causes a decrease of cell viability of 50%. All the reported values represent the means \pm SD of data derived from at least three independent experiments in duplicate.

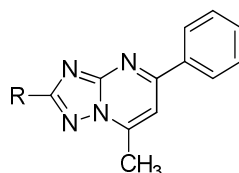
In the next step, on the basis of the biological results obtained, for all the compounds showing the ability to inhibit PA-PB1 interaction or both the PA-PB1 interaction and Flu replication (compounds **5**, **6** and **12-18**), the corresponding analogues functionalized with a 7-methyl-5-phenyl-[1,2,4]-triazolo[1,5-*a*]pyrimidine-2-carboxamide moiety were prepared. As shown in Table 2, the thienopyridine derivative **21** and benzothiazole derivative **25** showed an opposite profile to that exhibited by their isomers **12** and **17**. Indeed, both the compounds lost the ability to interfere with PA-PB1 heterodimerization but acquired some anti-Flu activity (EC₅₀ = 43 and 40 μ M, respectively), which however in compound **21** was coupled with cytotoxicity (CC₅₀ = 51 μ M). On the other hand, acid derivative **24** and tricyclic compound **26** showed good ability to inhibit PA-PB1 interaction (IC₅₀ = 18 and 15 μ M, respectively), with **26** exhibiting slightly higher anti-Flu activity (EC₅₀ = 40 μ M) than **24** (EC₅₀ = 70 μ M). A decreased anti-PA-PB1 activity was instead shown by thiophene derivative **22** (IC₅₀ = 50 μ M), which was also devoid of antiviral activity. Also

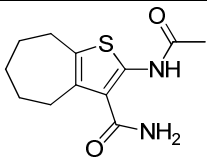
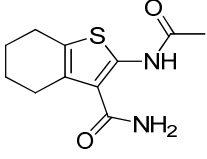
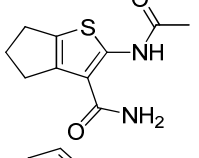
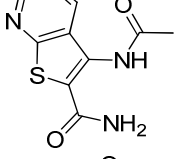
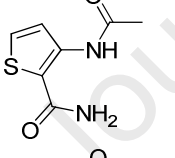
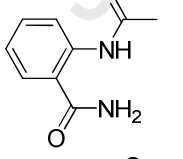
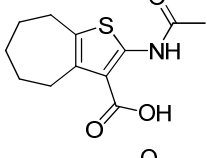
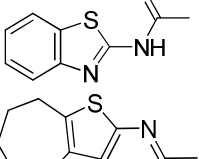
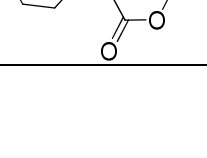
in this series, the cHTC could be favorably replaced by a phenyl ring, as shown by compound **23** [53] that, besides possessing very good anti-PA-PB1 activity ($IC_{50} = 7 \mu M$), also acquired interesting anti-Flu activity ($EC_{50} = 31 \mu M$) compared to its analogue **14** ($IC_{50} = 11 \mu M$ and $EC_{50} > 100 \mu M$).

In summary, the synthesis of novel hybrid compounds, aimed at clarifying the best substitution pattern for the C-2 position of the TZP ring, has led to the identification of some interesting compounds able to inhibit the PA-PB1 interaction and the viral growth. Interesting SAR insights have been outlined. In particular, the cHTC portion can be replaced by a benzene ring (as in compounds **14** and **23**), leading to a huge simplification also in terms of a chemical synthesis. The cycloheptathiophene moiety can be also favorably replaced by the tricyclic cycloheptathienooxazinone core (as in compounds **18** and **26**), which thus emerged as new scaffold able to ensure both anti-PA-PB1 and anti-Flu activity.

Among the synthesized derivatives, compounds **8**, **9**, **11**, **21** and **25** were able to interfere only with viral replication (EC_{50} s ranging from 15 to 49 μM). For these compounds, a different mechanism of action could be hypothesized, although none of them showed potent anti-Flu activity deserving mechanistic studies. On the other hand, compounds **12**, **14** and **17** showed the ability to disrupt PA-PB1 heterodimerization (IC_{50} s ranging from 3.3 to 50 μM) but no antiviral activity, leading to hypothesize an inappropriate pharmacokinetic profile. Thus, preliminary chemical/physical studies were performed for compound **14** and its isomer **23**, which was instead endowed with both anti-PA-PB1 and anti-Flu activities.

Table 2. Structure and Biological Activity of Compound **4** Analogues.



Compd	R	ELISA PA-PB1 Interaction Assay IC ₅₀ , μM ^a	PRA in MDCK cells EC ₅₀ , μM ^b	Cytotoxicity in MDCK cells CC ₅₀ , μM ^c
4		28 ± 1	8 ± 2	>250
19		N.D. ^d	N.D.	N.D.
20		N.D.	N.D.	N.D.
21		>200	43 ± 7	51 ± 1
22		50 ± 28	>100	240 ± 8
23		7 ± 1	31 ± 10	>250
24		18 ± 11	70 ± 15	>250
25		>200	40 ± 13	233 ± 5
26		15 ± 5	40 ± 6	>50
RBV			10 ± 2	>250

Tat-PB1₁₋₁₅ peptide	35 ± 4	41 ± 5	>100
---	--------	--------	------

For the definition of ^aIC₅₀, ^bEC₅₀, and ^cCC₅₀, see Table 1. ^dN.D. = not determined due to solubility issues.

2.3. Chemical-physical properties determination for compounds **14** and **23**

Trying to investigate as to why some compounds were able to interfere with PA-PB1 interface in the micromolar range while not showing anti-Flu activity, some preliminary chemical-physical properties were determined. To this aim, we selected the couple of regioisomer **14** and **23** both showing very good and comparable ability to inhibit PA-PB1 interaction (IC₅₀ = 11 and 7 μM, respectively) but only **23** showing anti-Flu activity (EC₅₀ = 31 μM).

First, we wished to exclude the hypothesis that the activity shown by compound **14** could be related to an artefact. Various mechanisms of assay interference or promiscuous behaviour have been described as responsible for Pan-Assay Interference Compounds (PAINS) activity, including chemical aggregation [54]. To test this hypothesis, compounds **14** and **23** were examined by using the ZINC15 remover filter (<http://zinc15.docking.org/patterns/home/>) [55] and none of them were found as potential aggregators or PAINS.

We next hypothesized that, in the case of compound **14**, solubility issues could have compromised the antiviral evaluation. Indeed, similarly to PPI inhibitors reported in the literature that are generally planar and hydrophobic molecules, the PA-PB1 inhibitors developed by us often suffered from poor solubility, as already highlighted for compounds **3** and **4** [32]. Thus, we evaluated the equilibrium solubility in phosphate buffer at pH 7.4 for the two isomers. Briefly, stock solutions (10⁻² M) of the compounds in DMSO were diluted to decreased molarity, from 300 μM to 0.1 μM, in 384 well transparent plate (Greiner 781801) with 1% DMSO: 99% PBS buffer, incubated at 37 °C and read after 2 hours in a NEPHELOstar Plus (BMG LABTECH). The results were adjusted to a segmented regression to obtain the maximum concentration in which compounds are soluble.

Compound **23** exhibited a higher equilibrium solubility (82.2 μM , 30.60 $\mu\text{g/mL}$) than **14** (17.6 μM , 6.55 $\mu\text{g/mL}$), suggesting that the low solubility of **14** could be at the basis of its inactivity in PRA assay.

Since the solubility of a molecule is a result of the dissociation from its crystal unit cell and the hydration once in solution, we investigated both these properties for the two isomers. In particular, in order to understand whether the difference in solubility shown by the compounds could originate by a different hydration, we calculated the Log Po/w value (average of five predictions calculated by using <http://www.swissadme.ch/>) [56] for **14** and **23**. Compounds showing poor solubility by poor hydration are referred to as ‘greaseball’ molecules and LogP values of 2-3 are considered as the cut-off point for hydration becoming a significant limitation for solubility [57]. Compounds **14** and **23** showed Log Po/w values of 2.15 and 2.07, respectively, suggesting that their different solubility was not originating from the degree of polarity and related solvation.

Then, we sought to investigate whether their different solubility in aqueous solvent could be dependent from the crystal lattice. Indeed, compounds with a strong crystal lattice, commonly referred to as ‘brick dust’ molecules, often show a limited capacity to dissociate from the solid form [58]. To this aim, we performed X-Ray analysis for the two isomers. Single crystals of **14** and **23** suitable for X-Ray analysis were obtained by crystallization by EtOH/DMF. The Ortep drawings of the asymmetric unit of the crystal structures are shown in Figure 3. Compound **14** crystallized in the Triclinic space group P-1 with unit cell parameters: $a = 6.412(2) \text{ \AA}$, $b = 8.167(2) \text{ \AA}$, $c = 16.243(5) \text{ \AA}$, $b \perp c$ 90.63(3), $\alpha = 88.374(11)^\circ$, $\beta = 87.191(11)^\circ$, $\gamma = 85.292(12)^\circ$, $V = 846.5(4) \text{ \AA}^3$, $Z = 2$, while compound **23** crystallized Monoclinic space group P 2(1)/n with unit cell parameters: $a = 7.9084(4) \text{ \AA}$, $b = 16.8578(13) \text{ \AA}$, $c = 12.4907(10) \text{ \AA}$, $b \perp c$ 90.63(3), $\alpha = \gamma = 90^\circ$, $\beta = 91.014(3)^\circ$, $\gamma = 85.292(12)^\circ$, $V = 1665.0(2) \text{ \AA}^3$ and $Z = 4$. The other structural details are given in the supporting information (**Tables S1** and **S2**). The solution and the refinement of the crystal structures of the two compounds allowed us to highlight similarities and differences of the two species in the solid state. In both cases, the configuration of the molecule is the same with the terminal amide group pointing

in the same direction with respect to the NH moiety of the secondary amide due to the presence of an intramolecular hydrogen bond between O1 and H2N. On the contrary, the dihedral angle involving the atoms C6-C7-N2-C8 (2.64° for **14**, 27.10° for **23**) and the torsion angle of the phenyl substituent with respect to the plane of the pyrimidine ring (35.46° for **14**, 11.88° for **23**) are relevantly different due to the presence of selective weak interactions that stabilize the two crystal structures. Particularly, the distortion of the structure of **23** is caused by the presence of a relatively strong intermolecular hydrogen bond between H1Nb and N3 (2.275 \AA), while the phenyl substituent on **14** is involved in multiple intermolecular π interactions with the phenyl moieties of other molecules of **14** causing a parallel displaced $\pi - \pi$ stacking (planes distance 3.710 \AA , centroids distance 4.072 \AA) [59], which provides a stabilization of the three-dimensional crystal lattice. In the latter case thus, the molecular packing can be attributed also to the formation of favorable interactions between neighboring aromatic side chains. The established interactions and consequently the different molecular packing may account for a substantial amount of the crystal stabilization. Accordingly, as they account for many characteristics of compounds, such as solubility, these features may justify the differences into the solubility values for compounds **14** and **23**, which could have compromised the antiviral evaluation.

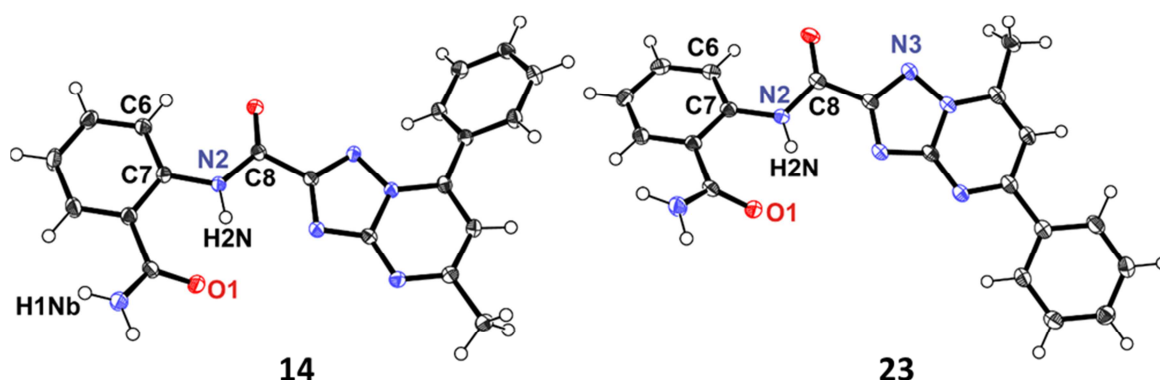


Figure 3. Asymmetric unit of **14** and **23**, showing a partial atom-numbering scheme. Displacement ellipsoids are drawn at 50% probability level.

2.4. In depth characterization of compound 23

2.4.1. Inhibition of Flu RdRP activity in a minireplicon assay

Then we investigated whether the compound ability to disrupt the PA–PB1 interaction *in vitro* correlated with the ability to interfere with the catalytic activity of FluA RdRP in a cellular context, by disrupting the correct assembly of the polymerase complex. To this aim, a minireplicon assay was performed for compound **23**. 293T cells were co-transfected with plasmids for the expression of FluA nucleoprotein (NP), PA, PB1, and PB2 proteins and the firefly luciferase RNA, flanked by the noncoding regions of Flu A/WSN/33 segment 8, in the presence of the test compound or DMSO as a control. The expression of the firefly reporter gene indicates that a negative-sense RNA is synthesized and is reconstituted intracellularly into functional vRNP in which all four NP, PA, PB1, and PB2 proteins are co-expressed and interact with each other. Compound **23** exhibited a potent inhibitory effect on FluA polymerase activity, showing an EC₅₀ of $5.8 \pm 2.0 \mu\text{M}$, and thus being more effective than RBV ($24 \pm 4 \mu\text{M}$). These data confirmed the ability of compound **23** to inhibit RdRP functions by interfering with PA-PB1 heterodimerization.

2.4.2. Metabolic stability in human liver microsomes

Metabolic stability in human liver microsomes (HLM) was studied by monitoring the percentage of unchanged substrate and the formation of the metabolite(s) at five time points (0, 10, 20, 40 and 60 min). LC-MS raw data were analyzed by using Mass-Metasite (version 3.3.6; Molecular Discovery Ltd., Middlesex, UK) [60,61] and WebMetabase (version 4.0.6; Molecular Discovery Ltd., Middlesex, UK) [62,63] software for automatic metabolite identification and structure elucidation as well as for kinetic analysis. After 60 min incubation, the 76% of compound **23** was in its unchanged form, indicating a good metabolic stability. In addition, the kinetic analysis performed in WebMetabase allowed to estimate the half-life value and the intrinsic clearance for compound **23**, as 166 min and $4.18 \mu\text{L}/\text{min} \cdot \text{mg}_{\text{prot}}$, respectively (**Figure S1**, supporting information). The analysis of formed metabolites allowed for the detection of one metabolite only, obtained by an aromatic hydroxylation reaction at the 2-carboxybenzamide moiety (**Figure S2**, supporting information).

Although the MS/MS fragmentation is not sufficient to identify the exact position of the site of metabolism in the aromatic ring, the most probable site for hydroxylation appears to be at C-4 position, according to MetaSite [64] predictions within the WebMetabase analysis tool (**Table S3** and **Figure S3**, supporting information).

2.4.3. Human plasma protein binding

Regarding the human plasma protein binding, samples were analyzed by employing a rapid equilibrium system device and adding them in buffer and measuring the compound presence in the human plasma compartment after 4 h of incubation by means of UPLC/MS/MS. It was observed that compound **23** showed an unbound fraction of 22.45%, which together with the good metabolic stability predicts a good bioavailability of the compound in human plasma.

2.4.4. Computational studies

Finally, with the aim to gain information on how two different moieties, such as the cHTC and the 2-carbamoylphenyl, showed a favorable ability to disrupt PA-PB1 interaction, computational studies were performed to predict the binding mode of benzamide derivative **23** within the PA cavity with respect to hit compound **4**. For comparative purpose, also its isomer **14**, which was active in ELISA-based assay but devoid of any antiviral activity, was studied in comparison to hit compound **3**.

The study was conducted using the same method applied for the evaluation of the binding mode of compounds **3** and **4** using the FLAP software [65], and the most probable binding poses for the two isomers are illustrated in **Figure 4**. In agreement with the biological results, both compounds showed an efficient binding within the PA_C, although through different orientations and interactions. In particular, both compounds were found to efficiently interact with W706 through hydrophobic interactions, as observed for all the inhibitors of the PA-PB1 interaction we have studied so far [24].

Similarly to **4**, compound **23** displayed a favorable hydrophobic interaction with all the three hydrophobic regions previously described by Liu and Yao [35]. Indeed, according to the proposed

description of the protein cavity, the first hydrophobic region is centered on residues W706 and F411, the second one is defined by F710 and L666, and the third one includes L640, V636, M595, and W619. However, differently from **4**, **23** seems to be involved in the formation of a favorable H-bond between the 2-carboxamide NH group and the hydroxyl group of T639. This amino acid was not found to be involved in such kind of interaction in other compounds studied so far by us.

Concerning compound **14**, the hydrophobic interaction occurs only in the first hydrophobic pocket, in a similar fashion to **3**. Differently from **3**, a favored H-bonding with Q408 was established with the 2-carboxamide carbonyl group instead of the carbonyl group of the amide linking the TZP and the phenyl ring. However, according to the GRID fields analysis in FLAP, for **14** the replacement of the cycloheptathiophene moiety with the phenyl ring led to a slightly different orientation that facilitates the formation of a second H-bond with I621, one of the key residues of PA in binding of PB1 (data not shown). Nevertheless, this slight change in the pose results in a reduced π - π interaction. This data seems to confirm the importance of an efficient interaction with W706 for inhibition of PA-PB1 heterodimerization.

In conclusion, the computational study confirmed the central interaction between the inhibitors and W706, and the 2-carboxamide group of **23** and **14** was pivotal in the interaction with PA by establishing favorable H-bonds. This is also experimentally confirmed, since the analogues lacking the 2-carboxamide substituent showed a very weak activity in the ELISA PA-PB1 interaction assays [32].

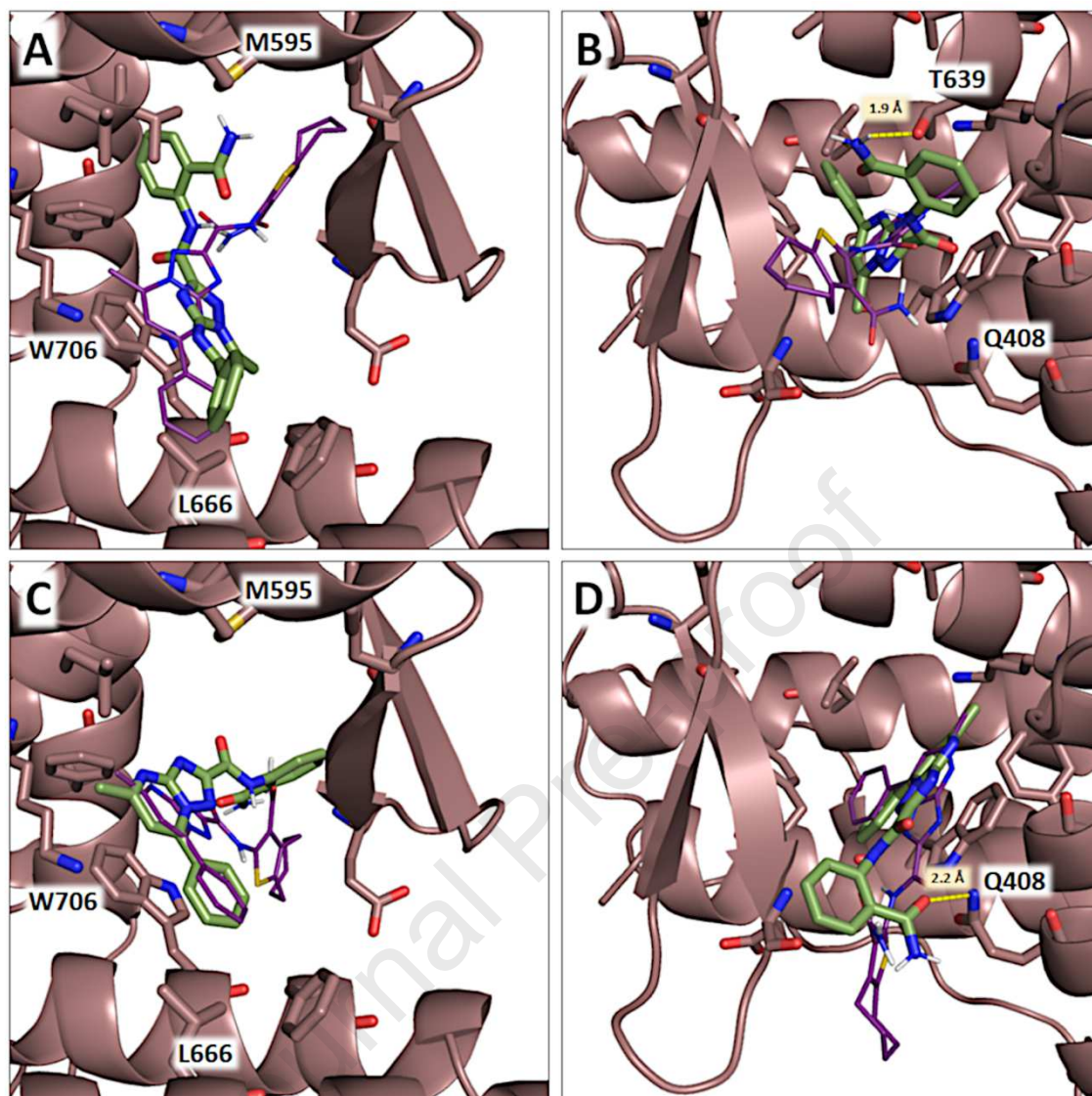


Figure 4. FLAP binding poses for compounds **23** (A,B) and **14** (C,D). Two orientations of the same pose in the PA cavity are illustrated to better visualize the predicted interactions. Compounds **14** and **23** are shown in sticks mode and in green color, while reference compounds **3** and **4** are shown in lines style and purple color.

3. Conclusions

The Flu RdRP is emerging as a privileged drug-target as demonstrated by the most recently approved compounds or in the pipeline such as favipiravir, baloxavir marboxil and pimodivir, which act by inhibiting each of the three RdRP subunits.

By applying an alternative approach to inhibit Flu RdRP functions, since many years we have been working on the development of compounds able to interfere with RdRP subunits interaction and in

particular with PA-PB1 heterodimerization. cHTC and TZP emerged among the best scaffolds able to disrupt this interaction, and their merging led us to identify interesting hybrid compounds (**3** and **4**). Starting from these hits, in this work, two sets of analogues were synthesized by maintaining the TZP core while deeply modifying the cHTC moiety. Some promising compounds showed the ability to interfere with the PA-PB1 interaction, such as cyclopentathiophene derivative **6** ($IC_{50} = 6.2 \mu\text{M}$), phenyl derivative **23** ($IC_{50} = 7 \mu\text{M}$) and cycloheptathienooxazinones **18** and **26** ($IC_{50} = 19$ and $15 \mu\text{M}$, respectively), coupled with good anti-Flu activity (EC_{50} ranging from 22 to $40 \mu\text{M}$). On the other hand, some compounds showed only anti-Flu activity ($EC_{50} = 15 - 50 \mu\text{M}$) leading to hypothesize a different mechanism of action, or only anti-PA-PB1 activity ($IC_{50} = 3.3 - 50 \mu\text{M}$). To investigate this latter behavior, chemical/physical properties were determined for the couple of isomers **14** and **23** both showing anti-PA-PB1 activity but only **23** having anti-Flu properties. Compound **14** showed a lower equilibrium solubility with respect to **23**, which could arise from a major molecular packing, as shown by X-Ray studies, which may account for a substantial amount of the crystal stabilization. In particular, the phenyl ring at the C-7 position of the TZP nucleus is involved in multiple intermolecular π - π interactions with the phenyl moieties of other molecules causing stabilization of the three-dimensional crystal lattice. These data confirmed one of the main drawbacks of PPI inhibitors that, interacting with interfaces generally flat and highly hydrophobic, often suffer from low solubility. In agreement, the PA_C cavity is characterized by hydrophobic regions and hydrophobic interactions are indispensable to achieve an efficient small molecule-PA binding. Computational studies performed on compounds **14** and **23** confirmed the crucial hydrophobic interaction between the TZP core and W706 for inhibition of PA-PB1 heterodimerization. Nevertheless, favorable H-bonds seem to contribute to the interaction of the compounds with the PA_C .

This work furnished important structure insights that could be exploited for the design of further analogues, also endowed with better drug-like properties. Indeed, the good biological and chemical/physical properties shown by compound **23**, in which a simpler phenyl ring replaced the

cycloheptathiophene, highlighted the possibility to reduce unnecessary hydrophobic moieties. A further increase of the hydrophilicity of the compounds could be also achieved by a structure-based drug design aimed at introducing polar groups establishing favorable H-bonds with the P_AC.

4. Experimental section

4.1. Chemistry

Commercially available starting materials, reagents, and solvents were used as supplied. All reactions were routinely monitored by TLC on silica gel 60F254 (Merck) and visualized by using UV or iodine. Flash column chromatography was performed on Merck silica gel 60 (mesh 230-400). After extraction, organic solutions were dried over anhydrous Na₂SO₄, filtered, and concentrated with a Büchi rotary evaporator at reduced pressure. Yields are of purified product and were not optimized. HRMS spectra were registered on Agilent Technologies 6540 UHD Accurate Mass Q-TOF LC/MS, HPLC 1290 Infinity. Purities of target compounds were determined by HPLC Waters LC Module I Plus and evaluated to be higher than 95% (at both 254 (reported below in the description of the compounds) and 296 nm). In order to evaluate their stability, the purity was also determined by HPLC analysis monitored at 296 nm after eleven days, and it was over 95%. HPLC conditions to assess the purity of final compounds were as follows: column: XTerra MS C18 column reversed-phase (3.5 μ spherical hybrid, 4.6 mm x 150 mm, 3.5 μm particle size); flow rate, 0.8 mL/min; acquisition time, 10 min; isocratic elution, mobile phase: acetonitrile 80%, water 20%, formic acid 0.1%. ¹H NMR and ¹³C NMR spectra were recorded on Bruker Avance DRX-400MHz using residual solvents such as dimethylsulfoxide (δ = 2.48) or chloroform (δ = 7.26) as an internal standard. Chemical shifts were recorded in ppm (δ) and the spectral data are consistent with the assigned structures. The spin multiplicities are indicated by the: symbols s (singlet), d (doublet), t (triplet), m (multiplet), and bs (broad singlet).

4.1.1. 2-Amino-6-ethyl-4,5,6,7-tetrahydrobenzo[*b*]thiophene-3-carboxamide (39). [40] A mixture of 4-ethylcyclohexanone (0.5 g, 3.96 mmol) 2-cyanoacetamide (0.35 g, 4.16 mmol) and

sulfur (0.13 g, 4.16 mmol) in ethanol (5 mL) was heated to reflux. Morpholine (0.36 g, 4.16 mmol) was added dropwise to the heating solution and the mixture was allowed to heat to reflux 4h. After cooling, the reaction mixture was poured into ice/water obtaining a precipitate which was filtered and treated with cyclohexane, to give **39** (0.7 g, 79%); ^1H NMR (DMSO- d_6 , 400 MHz): δ 0.86 (t, $J = 7.4$ Hz, 3H, CH_2CH_3), 1.16-1.35 (m, 4H, CH_2CH_3 and cyclohexane CH_2), 1.45-1.55, 1.77-1.80 and 2.00-2.06 (m, each 1H, cyclohexane CH), 2.51-2.57 (m, 2H, cyclohexane CH_2), 6.48 (bs, 2H, CONH_2), 6.86 (s, 2H, NH_2).

4.1.2. 2-Aminobenzo[*b*]thiophene-3-carboxamide (40). [41] A mixture of **36** [38] (0.5 g, 2.55 mmol) and *p*-chloroanil (1.25 g, 5.10 mmol) in 1,4-dioxane (30 mL) was heated at 90 °C for 4h. After cooling, the reaction mixture was filtered over celite and the filtrate was evaporated to dryness, to give a residue that was stirred with saturated NaHCO_3 solution for 15 min. The solution was then extracted with CH_2Cl_2 and the organic layers were evaporated to dryness to give a grey solid, which was purified by flash chromatography eluting with $\text{MeOH}/\text{CH}_2\text{Cl}_2$ (2%), to give **9** (0.29 g, 59%); ^1H NMR (DMSO- d_6 , 200 MHz): δ 6.80-6.95 (m, 3H, benzothiophene CH and NH_2), 7.15-7.20 (t, $J = 7.15$ Hz, 1H, benzothiophene CH), 7.50-7.60 (m, 4H, aromatic CH and CONH_2).

4.1.3. General procedure for carbodiimide formation (Method A). To a solution of 5-methyl-7-phenyl-[1,2,4]triazolo[1,5-*a*]pyrimidine-2-carboxylic acid [37] or 5-methyl-7-phenyl-[1,2,4]triazolo[1,5-*a*]pyrimidine-2-carboxylic acid [37] (1.0 equiv) in well dry CH_2Cl_2 , oxalyl chloride (3 equiv) was added and after 30 min dry DMF (2 drops) was added. After 2h, the reaction mixture was evaporated to dryness to give **30** [37] or **31** [37] that was dissolved in well dry CH_2Cl_2 and added of the appropriate amine (1.0 equiv) and DIPEA (1.0 equiv). The reaction mixture was maintained at r.t. until no starting material was detected by TLC. Then, it was worked up through two procedures: (procedure 1) the reaction mixture was evaporated to dryness to give a residue that was poured into ice/water providing a precipitate which was filtered and purified as reported in the description of the compounds; or (procedure 2) the precipitate formed in the reaction mixture was filtered and purified as reported in the description of the compounds.

4.1.4. *N*-(3-Carbamoyl-4,5,6,7-tetrahydrobenzo[*b*]thiophen-2-yl)-5-methyl-7-phenyl-[1,2,4]triazolo[1,5-*a*]pyrimidine-2-carboxamide (**5**). The title compound was prepared starting from **36** [38] and **30** [37] through method A (4h), worked up through procedure 1, and purified by flash chromatography eluting with MeOH/CHCl₃ (2%), in 57% yield as orange solid. ¹H NMR (DMSO-*d*₆, 400 MHz): δ 1.60-1.70 (m, 4H, cyclohexane CH₂), 2.40-2.75 (m, 7H, cyclohexane CH₂ and CH₃), 7.60-7.70 (m, 4H, phenyl CH and H-6), 8.10-8.20 (m, 2H, phenyl CH), 13.00 (s, 1H, NHCO); ¹³C NMR (DMSO-*d*₆, 101 MHz): δ 22.7, 22.8, 24.3, 25.3, 25.6, 112.3, 117.8, 127.6, 129.1, 129.7, 129.8, 130.0, 132.1, 141.7, 147.1, 155.7, 156.0, 157.6, 167.3, 167.6; HRMS: *m/z* calcd for C₂₂H₂₀N₆O₂S 433.1402 (M+H)⁺, found 433.144661 (M+H)⁺. HPLC, ret. time: 2.755 min, peak area: 98.70%.

4.1.5. *N*-(3-carbamoyl-5,6-dihydro-4*H*-cyclopenta[*b*]thiophen-2-yl)-5-methyl-7-phenyl-[1,2,4]triazolo[1,5-*a*]pyrimidine-2-carboxamide (**6**). The title compound was prepared starting from **37** [38] and **30** [37] through method A (4h), worked up through procedure 1, and purified by flash chromatography eluting with MeOH/CHCl₃ (2%), in 63% yield as yellow solid. ¹H NMR (DMSO-*d*₆, 400 MHz): δ 2.30-2.40 (m, 2H, cyclopentane CH₂), 2.70 (s, 3H, CH₃), 2.75-2.85 and 2.90-3.00 (m, each 2H, cyclopentane CH₂), 6.60 (bs, 1H, CONH₂), 7.55-7.70 (m, 5H, phenyl CH, H-6 and CONH₂), 8.10-8.20 (m, 2H, phenyl CH), 13.25 (s, 1H, NHCO); ¹³C NMR (DMSO-*d*₆, 101 MHz): δ 25.3, 28.1, 28.7, 29.4, 112.3, 112.9, 129.1, 129.7, 130.0, 132.2, 133.3, 139.9, 147.1, 147.3, 155.7, 156.0, 157.4, 167.3; HRMS: *m/z* calcd for C₂₁H₁₈N₆O₂S 419.1291 (M+H)⁺, found 419.128947 (M+H)⁺. HPLC, ret. time: 2.655 min, peak area: 99.12%.

4.1.6. *N*-(3-carbamoyl-4,5-dimethylthiophen-2-yl)-5-methyl-7-phenyl-[1,2,4]triazolo[1,5-*a*]pyrimidine-2-carboxamide (**7**). The title compound was prepared starting from **38** [66] and **30** [37] through method A (3h), worked up through procedure 1, and purified by flash chromatography eluting with MeOH/CHCl₃ (2%) and then washed with hot DMF, in 30% yield as yellow solid. ¹H NMR (DMSO-*d*₆, 200 MHz): δ 2.15 and 2.20 (s, each 3H, thiophene CH₃), 2.60 (s, 3H, CH₃), 7.60-7.70 (m, 4H, phenyl CH and H-6), 8.10-8.20 (m, 2H, phenyl CH), 12.75 (s, 1H, NHCO); ¹³C NMR

(DMSO-*d*₆, 101 MHz): δ 12.6, 13.8, 25.2, 112.3, 119.7, 124.5, 127.8, 129.1, 129.6, 129.9, 132.1, 139.9, 147.0, 155.6, 155.9, 157.4, 167.3, 167.7; HRMS: *m/z* calcd for C₂₀H₁₈N₆O₂S 407.1291 (M+H)⁺, found 407.12883 (M+H)⁺. HPLC, ret. time: 2.522 min, peak area: 95.37%.

4.1.7. *N*-(3-carbamoyl-6-ethyl-4,5,6,7-tetrahydrobenzo[*b*]thiophen-2-yl)-5-methyl-7-phenyl-[1,2,4]triazolo[1,5-*a*]pyrimidine-2-carboxamide (8). The title compound was prepared starting from **39** [40] and **30** [37] through method A (3h), worked up through procedure 1, and purified by flash chromatography eluting with MeOH/CHCl₃ (2%) and then treated with EtOH, in 60% yield as yellow solid. ¹H NMR (DMSO-*d*₆, 400 MHz): δ 0.90 (t, *J* = 7.3 Hz, 3H, CH₂CH₃), 1.30-1.40 (m, 3H, cyclohexane CH₂), 1.50-1.60, 1.80-1.90, and 2.20-2.30 (m, each 1H, cyclohexane CH₂), 2.65-2.75 (m, 6H, CH₂CH₃, cyclohexane CH, and CH₃), 7.50-7.60 (m, 6H, phenyl CH, H-6, and CONH₂), 8.10-8.20 (m, 2H, phenyl CH), 13.00 (s, 1H, NHCO); ¹³C NMR (DMSO-*d*₆, 101 MHz): δ 11.7, 25.2, 25.3, 28.4, 28.6, 30.2, 35.7, 112.2, 117.4, 127.3, 129.1, 129.6, 129.6, 129.9, 132.1, 141.8, 147.0, 155.6, 155.9, 157.4, 167.3, 167.5; HRMS: *m/z* calcd for C₂₄H₂₄N₆O₂S 461.1760 (M+H)⁺, found 461.175597 (M+H)⁺. HPLC, ret. time: 3.322 min, peak area: 96.12%.

4.1.8. *N*-(3-carbamoylbenzo[*b*]thiophen-2-yl)-5-methyl-7-phenyl-[1,2,4]triazolo[1,5-*a*]pyrimidine-2-carboxamide (9). The title compound was prepared starting from **40** [41] and **30** [37] through method A (1h), worked up through procedure 2, and purified by flash chromatography eluting with MeOH/CHCl₃ (2%), in 47% yield as yellow solid; ¹H NMR (DMSO-*d*₆, 400 MHz): δ 2.75 (s, 3H, CH₃), 7.30 and 7.45 (t, *J* = 7.5 Hz, each 1H, benzothiophene CH), 7.60-7.70 (m, 4H, phenyl CH and H-6), 7.85 (bs, 2H, CONH₂), 7.95-8.05 and 8.10-8.20 (m, each 2H, phenyl CH and benzothiophene CH), 13.50 (s, 1H, NHCO); ¹³C NMR (DMSO-*d*₆, 101 MHz): δ 25.2, 112.2, 112.4, 122.5, 122.9, 124.2, 125.7, 129.1, 129.5, 130.0, 132.2, 133.3, 134.0, 145.7, 147.1, 155.9, 156.8, 157.1, 167.3, 167.5; HRMS: *m/z* calcd for C₂₂H₁₆N₆O₂S 429.1134 (M+H)⁺, found 429.113549 (M+H)⁺. HPLC, ret. time: 2.633 min, peak area: 95.48%.

4.1.9. *N*-(3-carbamoyl-4,5,6,7-tetrahydrobenzo[*b*]thiophen-2-yl)-7-methyl-5-phenyl-[1,2,4]triazolo[1,5-*a*]pyrimidine-2-carboxamide (19). The title compound was prepared starting

from **36** [38] and **31** [37] through method A (overnight), worked up through procedure 2, and purified by flash chromatography eluting with MeOH/CHCl₃ (2%), in 30% yield as light yellow solid; ¹H NMR (DMSO-*d*₆, 400 MHz): δ 1.73-1.75 (m, 4H, cyclohexane CH₂), 2.60-2.65 and 2.70-2.75 (m, each 2H, cyclohexane CH₂), 2.85 (s, 3H, CH₃), 7.55-7.60 (m, 3H, phenyl CH), 8.10 (s, 1H, H-6), 8.25-8.30 (m, 2H, phenyl CH), 13.10 (s, 1H, NHCO); ¹³C NMR (DMSO-*d*₆, 101 MHz): δ 17.3, 22.7, 22.8, 24.2, 25.5, 109.2, 117.7, 127.6, 128.1, 129.5, 129.7, 132.0, 136.1, 141.6, 149.6, 155.2, 155.6, 157.9, 161.7, 167.5; HRMS: *m/z* calcd for C₂₂H₂₀N₆O₂S 433.1447 (M + H⁺), found 433.144794 (M+H)⁺. HPLC, ret. time: 2.806 min, peak area: 99.79%.

4.1.10. N-(3-carbamoyl-5,6-dihydro-4H-cyclopenta[*b*]thiophen-2-yl)-7-methyl-5-phenyl-[1,2,4]triazolo[1,5-*a*]pyrimidine-2-carboxamide (20). The title compound was prepared starting from **37** [38] and **31** [37] through method A (overnight), worked up through procedure 2, and purified by flash chromatography eluting with MeOH/CHCl₃ (2%), in 45% yield as yellow solid; ¹H NMR (DMSO-*d*₆, 400 MHz): δ 2.30 (quin, *J* = 7.2 Hz, 2H, cyclopentane CH₂), 2.80 (t, *J* = 7.2 Hz, 2H, cyclopentane CH₂), 2.85 (s, 3H, CH₃), 2.95 (t, *J* = 7.2 Hz, 2H, cyclopentane CH₂), 7.55-7.60 (m, 3H, phenyl CH), 8.05 (s, 1H, H-6), 8.25-8.30 (m, 2H, phenyl CH), 13.40 (s, 1H, NHCO); ¹³C NMR (DMSO-*d*₆, 101 MHz): δ 17.3, 28.1, 28.7, 29.5, 109.2, 117.7, 127.0, 128.1, 128.9, 129.5, 131.8, 133.4, 139.9, 149.5, 155.6, 156.4, 158.1, 162.0, 167.2; HRMS: *m/z* calcd for C₂₁H₁₈N₆O₂S 419.1291 (M+H)⁺, found 419.128962 (M+H)⁺. HPLC, ret. time: 3.069, peak area: 95.51%.

4.1.11. General procedure for hydrazide formation (Method B). A mixture of the appropriate reagent (0.5 g) and hydrazine hydrate (10 mL) was heated at 80 °C for 3h. After cooling, the precipitate obtained was filtered and washed with water.

4.1.12. 3-Amino-5,6,7,8-tetrahydro-4H-cyclohepta[*b*]thiophene-2-carbohydrazide (44). The title compound was prepared starting from **43** [45] through Method B in 99% yield; ¹H NMR (CDCl₃, 400 MHz): δ 1.50-1.70 (m, 6H, cycloheptane CH₂), 2.40-2.45 (m, 2H, cycloheptane CH₂), 2.70-2.75 (m, 2H, cycloheptane CH₂), 3.70 (bs, 2H, NHNH₂), 5.60 (s, 2H, NH₂), 6.50 (s, 1H, NHNH₂).

4.1.13. General procedure for hydrazide reduction (Method C). A mixture of the appropriate hydrazine and a catalytic amount of Ni-Raney in DMF was heated at 90 °C for until no starting material was detected by TLC. After cooling, the reaction mixture was filtered over celite and the filtrate was evaporated to dryness to give a residue, which was purified as reported below in the description of the compounds.

4.1.14. 3-Amino-5,6,7,8-tetrahydro-4H-cyclohepta[b]thiophene-2-carboxamide (45). The title compound was prepared starting from **44** through Method C (3h), after purification by treatment with Et₂O, in 54% yield; ¹H NMR (DMSO-*d*₆, 200 MHz): δ 1.25-1.50 (m, 6H, cycloheptane CH₂), 1.60-1.75 (m, 2H, cycloheptane CH₂), 2.50-2.60 (m, 2H, cycloheptane CH₂), 6.30 (s, 2H, NH₂), 6.60 (s, 2H, CONH₂).

4.1.15. N-(2-Carbamoyl-5,6,7,8-tetrahydro-4H-cyclohepta[b]thiophen-3-yl)-5-methyl-7-phenyl-[1,2,4]triazolo[1,5-*a*]pyrimidine-2-carboxamide (10). The title compound was prepared starting from **45** and **30** [37] through Method A (overnight), worked up through procedure 1, and purified by flash chromatography eluting with acetone/CHCl₃ (30%), in 48% yield as yellow solid; ¹H NMR (DMSO-*d*₆, 400 MHz): δ 1.40-1.50, 1.55-1.65, 1.75-1.85 and 2.35-2.45 (m, each 2H, cycloheptane CH₂), 2.65 (s, 3H, CH₃), 2.70-2.80 (m, 2H, cycloheptane CH₂), 7.30 (bs, 2H, CONH₂), 7.50-7.70 (m, 4H, aromatic CH and H-6), 8.15-8.20 (m, 2H, aromatic CH) 10.75 (s, 1H, NHCO); ¹³C NMR (DMSO-*d*₆, 101 MHz): δ 25.3, 27.2, 28.0, 28.3, 30.7, 32.2, 79.5, 112.2, 124.1, 129.1, 129.7, 130.0, 132.1, 135.9, 136.8, 139.5, 142.7, 147.1, 155.9, 158.4, 158.6, 163.6, 167.2; HRMS: *m/z* calcd for C₂₃H₂₂N₆O₂S 447.1604 (M+H)⁺, found 447.16086 (M+H)⁺. HPLC, ret. time: 2.559 min, peak area: 96.88%.

4.1.16. 3-Aminobenzo[b]thiophene-2-carboxamide (48). [48] The title compound was prepared starting from **46** [46] through Method B providing **47** [47] in 72% yield, followed by Method C (4h, purification by treatment with Et₂O) in 46% yield; ¹H NMR (DMSO-*d*₆, 200 MHz): δ 6.95-7.00 (m, 4H, CONH₂ and NH₂), 7.25-7.40 (m, 2H, aromatic CH), 7.70 (d, *J* = 7.66 Hz, 1H, aromatic CH), 7.90 (d, *J* = 8.25 Hz, 1H, aromatic CH).

4.1.17. *N*-(2-carbamoylbenzo[*b*]thiophen-3-yl)-5-methyl-7-phenyl-[1,2,4]triazolo[1,5-*a*]pyrimidine-2-carboxamide (**11**). The title compound was prepared starting from **48** [48] and **30** [37] through Method A (4h), worked up through procedure 1, and purified by flash chromatography eluting with MeOH/CHCl₃ (2%), in 40% yield as yellow solid; ¹H NMR (DMSO-*d*₆, 400 MHz): δ 2.75 (s, 3H, CH₃), 7.40 (t, *J* = 7.6 Hz, 1H, aromatic CH), 7.45 (t, *J* = 7.1 Hz, 1H, aromatic CH), 7.60-7.70 (m, 3H, aromatic CH), 7.70 (s, 1H, H-6), 7.75 (d, *J* = 8.1 Hz, 1H, aromatic CH), 7.80 (bs, 2H, CONH₂), 8.00 (d, *J* = 8.1 Hz, 1H, aromatic CH), 8.15-8.20 (m, 2H, aromatic CH), 11.70 (bs, 1H, NHCO); ¹³C NMR (DMSO-*d*₆, 101 MHz): δ 25.3, 79.6, 112.3, 123.4, 125.0, 127.3, 128.2, 129.2, 129.7, 130.0, 131.7, 132.2, 135.2, 137.1, 147.1, 156.0, 158.4, 164.0, 167.2; HRMS: *m/z* calcd for C₂₂H₁₆N₆O₂S 429.1134 (M+H)⁺, found 429.112694 (M+H)⁺. HPLC, ret. time: 2.384 min, peak area: 99.97%.

4.1.18. **3-Aminothiophene-2-carboxamide (50)**. [49] The title compound was prepared starting from methyl 3-aminothiophene-2-carboxylate through Method B providing **49** [47] in 100% yield, followed by Method C (overnight, purification by treatment with Et₂O) in 20% yield; ¹H NMR (DMSO-*d*₆, 400 MHz): δ 6.38 (s, 2H, NH₂), 6.52 (d, *J* = 4.8 Hz, 1H, thiophene CH), 6.81 (s, 2H, NH₂), 7.32 (d, *J* = 4.8 Hz, 1H, thiophene CH).

4.1.19. *N*-(2-Carbamoylthiophen-3-yl)-5-methyl-7-phenyl-[1,2,4]triazolo[1,5-*a*]pyrimidine-2-carboxamide (**13**). The title compound was prepared starting from **50** [49] and **30** [37] through Method A (1h), worked up through procedure 1, and purified by flash chromatography eluting with MeOH/CHCl₃ (2%), in 38% yield as yellow solid; ¹H NMR (DMSO-*d*₆, 400 MHz): δ 2.70 (s, 1H, CH₃), 7.65-7.65 (m, 4H, aromatic CH and H-6), 7.80 and 8.10 (d, *J* = 5.4 Hz, each 1H, thiophene CH), 8.15-8.20 (m, 2H, aromatic CH), 12.70 (s, 1H, NHCO); ¹³C NMR (DMSO-*d*₆, 101 MHz): δ 25.2, 112.1, 114.9, 122.0, 127.2, 129.1, 129.6, 130.0, 132.1, 141.8, 147.0, 156.0, 156.4, 158.2, 165.6, 167.1; HRMS: *m/z* calcd for C₁₈H₁₄N₆O₂S 379.0977 (M+H)⁺, found 379.097525 (M+H)⁺. HPLC, ret. time: 2.317 min, peak area: 99.85%.

4.1.20. N-(2-Carbamoylthiophen-3-yl)-7-methyl-5-phenyl-[1,2,4]triazolo[1,5-a]pyrimidine-2-carboxamide (22). The title compound was prepared starting from **50** [49] and **31** [37] through Method A (overnight), worked up through procedure 1, and purified by flash chromatography eluting with MeOH/CHCl₃ (4%), in 36% yield as yellow solid; ¹H NMR (DMSO-*d*₆, 400 MHz): δ 2.80 (s, 1H, CH₃), 7.50-7.60 (m, 4H, aromatic CH and CONH₂), 7.80 (d, *J* = 5.3 Hz, 1H, thiophene CH), 8.10 (s, 1H, H-6), 8.15 (d, *J* = 5.3 Hz, 1H, thiophene CH), 8.25-8.30 (m, 3H, aromatic CH and CONH₂), 12.90 (s, 1H, NHCO); ¹³C NMR (DMSO-*d*₆, 101 MHz): δ 17.3, 109.1, 114.9, 122.1, 127.9, 128.1, 129.5, 132.0, 136.2, 141.8, 149.5, 155.3, 156.4, 158.7, 161.7, 165.6; HRMS: *m/z* calcd for C₁₈H₁₄N₆O₂S 379.0977 (M+H)⁺, found 379.09724. HPLC, ret. time: 4.093 min, peak area: 95.93%.

4.1.21. 3-(5-Methyl-7-phenyl-[1,2,4]triazolo[1,5-a]pyrimidine-2-carboxamido)thieno[2,3-*b*]pyridine-2-carboxamide (12). The title compound was prepared starting from **52** [50] and **30** [37] through Method A (overnight), worked up through procedure 1, and purified by flash chromatography eluting with MeOH/CHCl₃ (3%), in 60% yield as yellow solid; ¹H NMR (DMSO-*d*₆, 400 MHz): δ 2.70 (s, 3H, CH₃), 7.50 (dd, *J* = 4.6 and 8.3 Hz, 1H, aromatic CH), 7.60-7.65 (m, 3H, aromatic CH), 7.70 (s, 1H, H-6), 7.95 (bs, 2H, CONH₂), 8.15-8.20 (m, 2H, aromatic CH), 8.30 (dd, *J* = 1.6 and 8.3 Hz, 1H, aromatic CH), 8.65 (dd, *J* = 1.6 Hz and 4.4 Hz, 1H, aromatic CH), 11.70 (s, 1H, NHCO); ¹³C NMR (DMSO-*d*₆, 101 MHz): δ 25.3, 112.3, 120.5, 124.9, 128.7, 129.2, 129.7, 130.0, 131.0, 132.2, 134.2, 147.1, 149.9, 156.1, 157.8, 158.1, 158.2, 164.1, 167.3; HRMS: *m/z* calcd for C₂₁H₁₅N₇O₂S 430.1087 (M+H)⁺, found 430.108031 (M+H)⁺. HPLC, ret. time: 2.284 min, peak area: 97.41%.

4.1.22. 3-(7-Methyl-5-phenyl-[1,2,4]triazolo[1,5-a]pyrimidine-2-carboxamido)thieno[2,3-*b*]pyridine-2-carboxamide (21). The title compound was prepared starting from **52** [50] and **31** [37] through Method A (1h), worked up through procedure 2, and purified by flash chromatography eluting with MeOH/CHCl₃ (5%), in 54% yield as yellow solid; ¹H NMR (DMSO-*d*₆, 400 MHz): δ 2.85 (s, 3H, CH₃), 7.50-7.55 (m, 1H, aromatic CH), 7.60-7.65 (m, 3H, aromatic CH), 7.70 (bs, 2H,

CONH₂), 8.15 (s, 1H, H-6), 8.30-8.35 (m, 3H, aromatic CH), 8.70-8.75 (m, 1H, aromatic CH), 11.70 (s, 1H, NHCO); ¹³C NMR (DMSO-*d*₆, 101 MHz): δ 17.3, 109.2, 120.5, 125.4, 128.1, 128.7, 129.5, 130.7, 132.0, 134.1, 136.1, 149.6, 149.8, 155.3, 157.7, 158.1, 158.6, 161.7, 163.9; HRMS: *m/z* calcd for C₂₁H₁₅N₇O₂S 430.1087 (M+H)⁺, found 430.108391 (M+H)⁺. HPLC, ret. time: 2.319 min, peak area: 96.26%.

4.1.23. 5-Methyl-7-phenyl-N-(3-(pyridin-2-ylcarbamoyl)-5,6,7,8-tetrahydro-4H-cyclohepta[b]thiophen-2-yl)-[1,2,4]triazolo[1,5-a]pyrimidine-2-carboxamide (16). The title compound was prepared starting from **53** [29] and **30** [37] through Method A (overnight), worked up through procedure 1, and purified by treatment with Et₂O, in 97% yield as yellow solid. ¹H NMR (DMSO-*d*₆, 400 MHz): δ 1.50-1.70 (m, 4H, cycloheptane CH₂), 1.75-1.85 (m, 2H, cycloheptane CH₂), 2.65 (s, 3H, CH₃), 2.70-2.75 and 2.80-2.85 (m, each 2H, cycloheptane CH₂), 7.15-7.20 (m, 1H, aromatic CH), 7.55-7.70 (m, 4H, aromatic CH and H-6), 7.80-7.85 (m, 1H, aromatic CH), 8.10-8.15 (m, 2H, aromatic CH), 8.20-8.25 and 8.30-8.35 (m, each 1H, aromatic CH), 10.25 and 11.50 (s, each 1H, NHCO); ¹³C NMR (DMSO-*d*₆, 101 MHz): δ 25.2, 27.3, 27.8, 28.7, 31.9, 112.3, 115.0, 120.4, 123.0, 129.0, 129.6, 129.9, 132.1, 132.2, 135.9, 136.8, 138.5, 147.1, 148.5, 151.9, 155.8, 155.9, 157.3, 164.7, 167.4; HRMS: *m/z* calcd for C₂₈H₂₅N₇O₂S 524.1869 (M+H)⁺, found 524.186282 (M+H)⁺. HPLC, ret. time: 4.344 min, peak area: 98.46%.

4.1.24. Ethyl 2-(5-methyl-7-phenyl-[1,2,4]triazolo[1,5-a]pyrimidine-2-carboxamido)-5,6,7,8-tetrahydro-4H-cyclohepta[b]thiophene-3-carboxylate (55). The title compound was prepared starting from **54** [52] and **30** [37] through Method A (1h), worked up through procedure 1, and purified by flash chromatography eluting with acetone/CHCl₃ (5%), in 61% yield; ¹H NMR (DMSO-*d*₆, 400 MHz): δ 1.30 (t, *J* = 7.1 Hz, 3H, CH₂CH₃), 1.50-1.65 (m, 4H, cycloheptane CH₂), 1.70-1.80 (m, 2H, cycloheptane CH₂), 2.65-2.75 (m, 5H, cycloheptane CH₂ and CH₃), 3.00-3.10 (m, 2H, cycloheptane CH₂), 4.30 (q, *J* = 7.1 Hz, 2H, CH₂CH₃), 7.55-7.70 (m, 4H, aromatic CH and H-6), 8.10-8.20 (m, 2H, aromatic CH), 12.40 (s, 1H, NHCO).

4.1.25. Ethyl 2-(7-methyl-5-phenyl-[1,2,4]triazolo[1,5-*a*]pyrimidine-2-carboxamido)-5,6,7,8-tetrahydro-4*H*-cyclohepta[*b*]thiophene-3-carboxylate (56). The title compound was prepared starting from **54** [52] and **31** [37] through Method A (1h), worked up through procedure 2, and purified by treatment by EtOAc/EtOH mixture, in 56% yield; ¹H NMR (DMSO-*d*₆, 400 MHz): δ 1.30 (t, *J* = 7.1 Hz, 3H, CH₂CH₃), 1.50-1.65 (m, 4H, cycloheptane CH₂), 1.70-1.80 (m, 2H, cycloheptane CH₂), 2.65-2.70 (m, 2H, cycloheptane CH₂), 2.80 (s, 3H, CH₃), 2.90-3.00 (m, 2H, cycloheptane CH₂), 4.30 (q, *J* = 7.1 Hz, 2H, CH₂CH₃), 7.55-7.60 (m, 3H, aromatic CH), 8.05 (s, 1H, H-6), 8.20-8.25 (m, 2H, aromatic CH), 12.40 (s, 1H, NHCO).

4.1.26. 2-(5-Methyl-7-phenyl-[1,2,4]triazolo[1,5-*a*]pyrimidine-2-carboxamido)-5,6,7,8-tetrahydro-4*H*-cyclohepta[*b*]thiophene-3-carboxylic acid (15). A suspension of **55** (0.33 g, 0.69 mmol) and LiOH (0.11 g, 2.77 mmol) in a mixture H₂O/THF (1:1) was maintained at 50 °C for 24h. After cooling the reaction mixture was acidified (pH 4-5) with 2N HCl obtaining a precipitate that was filtered and purified by flash chromatography eluting with MeOH/CHCl₃ (3%) to give **15** (0.25 g, 80% yield) as yellow solid; ¹H NMR (DMSO-*d*₆, 400 MHz): δ 1.35-1.60 (m, 4H, cycloheptane CH₂), 1.70-1.80 (m, 2H, cycloheptane CH₂), 2.60-2.70 (m, 5H, cycloheptane CH₂ and CH₃), 3.20-3.30 (m, 2H, cycloheptane CH₂), 7.60-7.70 (m, 4H, aromatic CH and H-6), 8.10-8.20 (m, 2H, aromatic CH), 14.50 (bs, 1H, COOH); ¹³C NMR (DMSO-*d*₆, 101 MHz): δ 25.2, 27.3, 27.7, 28.3, 28.8, 32.8, 112.0, 121.0, 129.1, 129.7, 130.0, 130.1, 132.1, 139.0, 140.4, 147.0, 155.5, 155.9, 158.4, 167.0; HRMS: *m/z* calcd for C₂₃H₂₁N₅O₂S 448.14441 (M+H)⁺, found 448.143999 (M+H)⁺. HPLC, ret. time: 3.303 min, peak area: 98.83%.

4.1.27. 2-(7-Methyl-5-phenyl-[1,2,4]triazolo[1,5-*a*]pyrimidine-2-carboxamido)-5,6,7,8-tetrahydro-4*H*-cyclohepta[*b*]thiophene-3-carboxylic acid (24). The title compound was prepared starting from **56** through the procedure used for the synthesis of **15** in 58% yield; ¹H NMR (DMSO-*d*₆, 400 MHz): δ 1.50-1.55 (m, 4H, cycloheptane CH₂), 1.75-1.80 and 2.65-2.70 (m, each 2H, cycloheptane CH₂), 2.85 (s, 3H, CH₃), 3.05-3.10 (m, 2H, cycloheptane CH₂), 7.60-7.70 (m, 3H, aromatic CH), 8.10 (s, 1H, H-6), 8.20-8.25 (m, 2H, aromatic CH). ¹³C NMR (DMSO-*d*₆, 101

MHz): δ 17.3, 27.2, 27.5, 27.9, 28.5, 32.3, 109.1, 122.1, 128.0, 129.5, 131.2, 132.0, 135.6, 136.1, 138.0, 149.5, 155.2, 155.6, 158.0, 161.8, 167.5. HRMS: m/z calcd for $C_{23}H_{21}N_5O_3S$ 448.14441 ($M+H$)⁺, found 448.14375 ($M+H$)⁺. HPLC, ret. time: 5.832 min, peak area: 100%.

4.1.28. 2-(5-Methyl-7-phenyl[1,2,4]triazolo[1,5-*a*]pyrimidin-2-yl)-6,7,8,9-tetrahydro-4*H*,5*H*-cyclohepta[4,5]thieno[2,3-*d*][1,3]oxazin-4-one (18). A mixture of **15** (0.33 g, 0.73 mmol) and acetic anhydride (0.78 g, 7.7 mmol) was heated at 100 °C for 30 h. After cooling, the reaction mixture was poured into ice/water obtaining a precipitate that was filtered and crystallized by EtOH/DMF, to give **18** (0.06 g, 19%); ¹H-NMR (DMSO-*d*₆) δ : 1.60-1.65 (m, 4H, cycloheptane CH₂), 1.80-1.85 (m, 2H, cycloheptane CH₂), 2.70 (s, 3H, CH₃), 2.85-2.90 and 3.10-3.15 (m, each 2H, cycloheptane CH₂), 7.60-7.65 (m, 4H, H-6 and aromatic CH), 8.10-8.15 (m, 2H, aromatic CH); ¹³C-NMR (101 MHz, DMSO-*d*₆) δ : 25.2, 26.9, 27.5, 27.7, 29.5, 32.0, 112.4, 118.8, 129.1, 129.7, 129.8, 132.0, 137.9, 141.2, 146.9, 151.6, 154.7, 156.2, 156.6, 158.3, 167.2; HRMS: m/z calcd for $C_{23}H_{19}N_5O_2S$ 430.1338 ($M+H$)⁺, found 430.133443 ($M+H$)⁺. HPLC, ret. time: 3.875 min, peak area: 98.83%.

4.1.29. 2-(7-Methyl-5-phenyl[1,2,4]triazolo[1,5-*a*]pyrimidin-2-yl)-6,7,8,9-tetrahydro-4*H*,5*H*-cyclohepta[4,5]thieno[2,3-*d*][1,3]oxazin-4-one (26). To a suspension of **24** (0.04 g, 0.089 mmol) in dry CH₂Cl₂, a solution of EDC hydrochloride (0.017 g, 0.089 mmol), DMAP (0.011 g, 0.089 mmol), and HOBt monohydrate (0.013 g, 0.089 mmol) in CH₂Cl₂ was added dropwise at 0 °C. The reaction mixture was maintained at rt for 24h and, then, it was evaporated to dryness providing a residue that was purified by flash chromatography eluting with MeOH/CHCl₃ (2%), to give **26** (0.02 g, 52%); ¹H-NMR (DMSO-*d*₆) δ : 1.65-1.60 (m, 4H, cycloheptane CH₂), 1.80-1.85 (m, 2H, cycloheptane CH₂), 2.80-2.90 (m, 5H, cycloheptane CH₂ and CH₃), 3.10-3.15 (m, 2H, cycloheptane CH₂), 7.55-7.60 (m, 3H, aromatic CH), 8.10 (s, 1H, H-6), 8.25-8.30 (m, 2H, aromatic CH); ¹³C-NMR (101 MHz, DMSO-*d*₆) δ : 17.4, 26.9, 27.5, 27.7, 29.5, 32.0, 109.1, 118.8, 128.0, 129.6, 132.0, 136.1, 138.0, 141.3, 149.2, 151.6, 154.8, 156.9, 158.4, 161.5, 166.4; HRMS: m/z calcd for

$C_{23}H_{19}N_5O_2S$ 430.1338 (M+H)⁺, found 430.133652 (M+H)⁺. HPLC, ret. time: 3.652, peak area: 97.58%.

4.1.30. *N*-(benzo[*d*]thiazol-2-yl)-5-methyl-7-phenyl-[1,2,4]triazolo[1,5-*a*]pyrimidine-2-carboxamide (**17**). The title compound was prepared starting from 2-aminobenzothiazole and **30** [37] through Method A (72h), worked up through procedure 1, and purified by flash chromatography eluting with acetone/CHCl₃ (5%), in 36% yield as yellow solid; ¹H NMR (DMSO-*d*₆, 400 MHz): δ 2.70 (s, 3H, CH₃), 7.30 (t, *J* = 7.4 Hz, 1H, aromatic CH), 7.40 (t, *J* = 7.3 Hz, 1H, aromatic CH), 7.55-7.70 (m, 4H, aromatic CH and H-6), 7.80 (d, *J* = 7.9 Hz, 1H, aromatic CH), 8.10 (d, *J* = 7.7 Hz, 1H, aromatic CH), 8.20-8.30 (m, 2H, aromatic CH), 13.10 (bs, 1H, NHCO); ¹³C NMR (DMSO-*d*₆, 101 MHz): δ 25.3, 112.4, 121.0, 122.3, 124.5, 126.8, 129.2, 129.5, 130.1, 131.9, 132.2, 147.1, 156.1, 156.4, 157.6, 158.1, 159.4, 167.4; HRMS: *m/z* calcd for C₂₀H₁₁N₆OS 387.1029 (M+H)⁺, found 387.102196 (2M+H)⁺. HPLC, ret. time: 3.278 min, peak area: 98.8%.

4.1.31. *N*-(Benzo[*d*]thiazol-2-yl)-7-methyl-5-phenyl-[1,2,4]triazolo[1,5-*a*]pyrimidine-2-carboxamide (**25**). The title compound was prepared starting from 2-aminobenzothiazole and **31** [37] through Method A (72h), worked up through procedure 2, and purified by crystallization by DMF, in 57% yield as yellow solid; ¹H NMR (DMSO-*d*₆, 400 MHz): δ 2.85 (s, 1H, CH₃), 7.35 and 7.45 (t, *J* = 7.6 Hz, each 1H, aromatic CH), 7.55-7.60 (m, 3H, aromatic CH), 7.80 and 8.00 (d, *J* = 8.0 Hz, each 1H, aromatic CH), 8.10 (s, 1H, H-6), 8.25-8.30 (m, 2H, aromatic CH), 13.0 (s, 1H, NHCO); ¹³C NMR (DMSO-*d*₆, 101 MHz): δ 17.3, 109.3, 121.0, 122.2, 124.4, 126.7, 128.1, 129.5, 131.9, 132.0, 136.1, 148.3, 149.5, 155.3, 158.0, 151.1, 159.4, 161.8; HRMS: *m/z* calcd for C₂₀H₁₁N₆OS 387.1029 (M+H)⁺, found 387.1022 (M+H)⁺. HPLC, ret. time: 2.898 min, peak area: 99.85%.

4.2. Computational methods

The binding poses of compounds **23** and **14** in the PA cavity were generated using the FLAP software (version 2.2.1, Molecular Discovery Ltd., Middlesex, UK; www.moldiscovery.com); the procedure has been extensively described elsewhere [26,27,29]. The main cavity of the

crystallographic structure of a large C-terminal fragment of PA (aa 257-716) (pdb code: 3CM8) [21] was used as a template. A total of 50 conformers for each ligand was generated to mimic the compound flexibility, and the most abundant protonation state of each molecule was used, as predicted by MoKa [67]. The probes used to generate the GRID Molecular Interaction Fields were H (shape), DRY (hydrophobic interactions), N1 (H-bond donor) and O (H-bond acceptor) interactions.

4.3. Biology

4.3.1. Compounds and peptide

RBV (1-D-ribofuranosyl-1,2,4-triazole-3-carboxamide) was purchased from Roche. Each test compound was dissolved in 100% DMSO. The PB1₍₁₋₁₅₎-Tat peptide was synthesized and purified by the Peptide Facility of CRIBI Biotechnology Center (University of Padua, Padua, Italy). This peptide corresponds to the first 15 amino acids of PB1 protein fused to a short sequence of HIV Tat protein (amino acids 47–59), which allows the delivery into the cell [68].

4.3.2. Cells and Virus

Mardin-Darby canine kidney (MDCK) and human embryonic kidney (HEK) 293T cells were grown in Dulbecco's modified Eagle's medium (DMEM, Life Biotechnologies) supplemented with 10% (v/v) fetal bovine serum (FBS, Life Technologies) and antibiotics (100 U/mL penicillin and 100 µg/mL streptomycin, Life Technologies). Cells were maintained at 37 °C in a humidified atmosphere with 5% CO₂. Influenza virus strain A/PR/8/34 (H1N1, Cambridge lineage) was kindly provided by P. Digard (Roslin Institute, University of Edinburgh, United Kingdom).

4.3.3. PA-PB1 interaction enzyme-linked immunosorbent assay (ELISA)

The PA–PB1 interaction was detected by a procedure previously described [27]. Briefly, 96-well microtiter plates (Nuova Aptca) were coated with 400 ng of 6His-PA₍₂₃₉₋₇₁₆₎ for 3 h at 37 °C and then blocked with 2% BSA (Sigma) in PBS for 1 h at 37 °C. The 6His-PA₍₂₃₉₋₇₁₆₎ protein was expressed in *E. coli* strain BL21(DE3)pLysS and purified as already described [27]. After washing, 200 ng of GST-PB1₍₁₋₂₅₎, or of GST alone as a control, in the absence or the presence of test

compounds at various concentrations, were added and incubated O/N at room temperature. *Escherichia coli*-expressed, purified GST and GST-PB1₍₁₋₂₅₎ proteins were obtained as previously described [27,69]. After washing, the interaction between 6His-PA₍₂₃₉₋₇₁₆₎ and GST-PB1₍₁₋₂₅₎ was detected with a horseradish peroxidase-coupled anti-GST monoclonal antibody (GenScript) diluted 1:4,000 in PBS supplemented with 2% FBS. Following washes, the substrate 3,3',5,5'-tetramethylbenzidine (TMB, KPL) was added and absorbance was measured at 450 nm by an ELISA plate reader (Tecan Sunrise™). Values obtained from the samples treated with only DMSO were used to set as 100% of PA–PB1 interaction.

4.3.4. Cytotoxicity assay

Cytotoxicity of compounds was tested in MDCK cells by the 3-(4,5-dimethylthiazol-2-yl)-2,5-diphenyl tetrazolium bromide (MTT) method, as previously reported [27,70]. Briefly, MDCK cells (seeded at density of 2×10^4 per well) were grown in 96-well plates for 24 h and then treated with serial dilutions of test compounds, or DMSO as a control, in DMEM supplemented with 10% FBS. After incubation at 37 °C for 48 h, 5 mg/mL of MTT (Sigma) in PBS was added into each well and incubated at 37 °C for further 4 h. Successively, a solubilization solution was added to lyse the cells and incubated O/N at 37 °C. Finally, optical density was read at the wavelength of 620 nm on a microtiter plate reader (Tecan Sunrise™).

4.3.5. Plaque reduction assay (PRA)

The antiviral activity of test compounds against influenza A virus was tested by PRA as previously described [27]. MDCK cells were seeded at 5×10^5 cells/well into 12-well plates, and incubated at 37 °C for 24 h. The following day, the culture medium was removed and the monolayers were first washed with serum-free DMEM and then infected with the Flu A/PR/8/34 strain at 40 PFU/well in DMEM supplemented with 1 µg/mL of TPCK-treated trypsin (Worthington Biochemical Corporation) and 0.14% BSA and incubated for 1 h at 37 °C. The influenza virus infection was performed in the presence of different concentrations of test compounds or solvent (DMSO) as a control. After virus adsorption, DMEM containing 1 µg/mL of TPCK-treated trypsin, 0.14% BSA,

1.2% Avicel, and DMSO or test compounds was added to the cells. At 48 h post-infection, cells were fixed with 4% formaldehyde and stained with 0.1% toluidine blue. Viral plaques were counted, and the mean plaque number in the DMSO-treated control was set at 100%.

4.3.6. Minireplicon assays

The minireplicon assay was performed as described [27], with some modifications. Briefly, HEK 293T cells (2×10^5 cells per well) were plated into 24-well plates and incubated overnight at 37 °C. The next day, cells were transfected using calcium phosphate co-precipitation method with pcDNA-PB1, pcDNA-PB2, pcDNA-PA, pcDNA-NP plasmids (100 ng/well of each) along with 50 ng/well of the pPoli-Flu-ffLuc reporter plasmid and 50 ng/well of pRL-SV40 plasmid as a transfection control. Transfections were performed in the presence of different concentrations of test compounds or DMSO. RBV was used as a positive control for inhibition. Cell medium was removed 5 h post-transfection and replaced with DMEM containing the compounds, RBV, or DMSO. At 24 h post-transfection, cells were harvested, lysed and both firefly and *Renilla* luciferase activity were measured using the Dual Luciferase Assay Kit (Promega). In each experiment, firefly luciferase activity was normalized with that of the *Renilla* luciferase and relative luciferase units (RLU) were obtained. The activity measured in control transfection reactions containing DMSO was set at 100% of polymerase activity.

4.4. Equilibrium solubility assay

The stock solutions (10⁻² M) of the assayed compounds were diluted to decreased molarity, from 300 µM to 0.1µM, in 384 well transparent plate (Greiner 781801) with 1% DMSO: 99% PBS buffer. Then, they were incubate at 37 °C and read after 2 hours in a NEPHELOstar Plus (BMG LABTECH). The results were adjusted to a segmented regression to obtain the maximum concentration in which compounds are soluble. Digossin, prazosin and progesterone were used as reference compounds (equilibrium solubility = 84.0, 62.8 and 6.5 µM, respectively) [71].

4.5. X-Ray studies

X-Ray diffraction patterns of the crystals were recorded using a Bruker D8 Venture diffractometer equipped with an Incoatec ImuS3.0 microfocus sealed-tube Mo K α ($\lambda = 0.71073 \text{ \AA}$) source and a CCD Photon II detector. The analyses were carried out at 120 (2) K using an Oxford Cryosystems 800 cooler. The data collected through generic φ and ω were integrated and reduced using the Bruker AXS V8 Saint Software. The structures were solved and all the thermal parameters were anisotropically refined using the SHELXT and SHELXL packages of the Bruker APEX3 software.

4.6. Human plasma protein binding

The assay was carried out by employing Rapid Equilibrium Dialysis (RED) from Thermo Scientific. The compounds were dissolved at 5 μM in plasma (from Seralab) and added to the corresponding insert of the RED device. Dialysis buffer was added to the corresponding insert of the RED device. Plate was incubated for 4h at 37 $^{\circ}\text{C}$ and, then, 50 μL aliquots of each chamber were transferred to empty vials. 50 μL of dialysis buffer were added to the plasma samples and 50 μL of plasma were added to the buffer samples. 300 μL of acetonitrile were added to all the samples and centrifuged at 4000 rpm. Supernatant was taken and analyzed by UPLC/MS/MS for sample quantification. Stationary phase: Reverse phase Acquity UPLC $^{\circledR}$ BEH C18 1,7 μm (2.1 mm x 50 mm) (Waters); mobile phase: 0.1% Formic acid water/0.1% formic acid in acetonitrile; gradient:

Time	Water	Acetonitrile
0	95%	5%
0.1	95%	5%
1	0%	100%
2	0%	100%
2.1	95%	5%
2.5	95%	5%

Flow: 0.6 ml/min. The chromatographic equipment employed was an UPLC QSM Waters Acquity.

Compound concentrations were calculated from the MS peak areas.

4.7. Metabolic stability in human liver microsomes

Test compounds (10 μM) were preincubated for 5 min at 37 $^{\circ}\text{C}$ in a 0.1 M phosphate buffer (pH 7.4) containing Human Liver Microsomes (1 mg/mL) in a total volume of 500 μL . The reactions were initiated by addition of NADPH (2 mM) in a shaking water bath at 37 $^{\circ}\text{C}$. An aliquot of

reactions mixture (75 μ L) was taken at 0, 10, 20, 40 and 60 min and was added to 75 μ L of cold acetonitrile (containing 10 μ M labetalol as an internal standard) to terminate the reaction. Proteins were precipitated by centrifugation at 12 000g for 5 min at 4 °C (Eppendorf, Italy; centrifuge 5810 R; rotor F-45-30-11), and aliquots of the supernatants were analyzed by LC–MS/MS.

The instrumentation used in this study consisted in an Agilent 6540 UHD Accurate-Mass Quadrupole Time-of-Flight (QTOF), equipped with an Agilent 1290 Infinity LC system (Agilent Technologies, Santa Clara, CA, USA).

The columns was a Phenomenex Luna Omega Polar C18 column (1.6 μ m, 2.1 \times 150 mm). Column temperature was set at 40 °C and injection volume was 5 μ l. The mobile phases consisted of 0.1% formic acid in water (A) and acetonitrile + 0.1% formic acid (B) and the LC gradient was as follows: 0–10 min 0–95% B, 10-12 min 95-95% B, at a flow rate of 0.4 ml/min. The Agilent Technology 6540 UHD Accurate Mass Q-TOF LC/MS system was operated under positive conditions with Dual JetStream source (ESI source) in the following conditions: Gas Temp 350 °C, Drying Gas: 9 l/min, Nebulizer: 35 psi, Sheath Gas Temp: 400 °C, Sheath Gas Flow: 9 L/min, Vcap: 4000V, Nozzle Voltage: 0V, Fragmentor: 120V, Skimmer: 65V, OCT RF Vpp: 750V. The acquisition was performed in AutoMS/MS mode using a mass list to trigger the MS/MS acquisition based on the accurate masses of potential metabolites as computed by MetaSite software [64]. The AutoMS/MS settings were: MS range: 119 – 1400 m/z, rate 3 spectra/s; MS/MS range: 100 – 1400 m/z, Rate 6 spectra/s; Isolation Width: “medium (4 m/z); Fixed Collision energy 15V, max 1 precursor Per Cycle, Abs. Precursor threshold 100 counts, Rel Threshold 0.01%. Data Analysis was performed by processing raw data files using Mass-MetaSite (version 3.3.6, Molecular Discovery Ltd., Middlesex, UK, Molecular Discovery Ltd., UK; www.moldiscovery.com) and WebMetabase (version 4.0.6 Molecular Discovery Ltd., Middlesex, UK, Molecular Discovery Ltd., UK; www.moldiscovery.com).

Acknowledgments

This work was supported by grants “Excellent Departments” by Ministero dell’Istruzione, dell’Università e della Ricerca-MIUR (to S. Massari and A. Donnadio), PRIN 2017 - cod. 2017BMK8JR (to S. Massari, S. Sabatini, and V. Cecchetti), Fondazione Cassa Risparmio Perugia - Ricerca Scientifica e Tecnologica 2019: “Giovani ricercatori: risorsa per il territorio” (to M.C. Pismataro), Associazione Italiana per la Ricerca sul Cancro, AIRC – Fellowships for Italy 2018 (to T. Felicetti), Xunta de Galicia (ED431C 2018/21 & ED431G 2019/02), European Regional Development Fund (ERDF) (to J. Brea), Associazione Italiana per la Ricerca sul Cancro, AIRC, grant n. IG18855 (to A. Loregian); British Society for Antimicrobial Chemotherapy, UK, BSAC-2018-0064 (to A. Loregian), Ministero dell’Istruzione, dell’Università e della Ricerca, PRIN 2017 - cod. 2017KM79NN (to A. Loregian), Fondazione Cassa di Risparmio di Padova e Rovigo - Bando Ricerca Covid-2019 Nr. 55777 2020.0162 (to A. Loregian), and financial support to the project AMIS, through the program “Dipartimenti di Eccellenza 2018–2022, by Ministero dell’Istruzione, dell’Università e della Ricerca-MIUR-project AMIS (to L. Goracci and L. Tensi).

Supporting Information. Appendix A. Supplementary data

References

- [1] world health organization WHO, Influenza., <http://www.who.int/influenza> (accessed September 4, 2020).
- [2] J.K. Taubenberger, J.C. Kash, D.M. Morens, The 1918 influenza pandemic: 100 years of questions answered and unanswered, *Sci. Transl. Med.* 11 (2019) 5485–5501. <https://doi.org/10.1126/scitranslmed.aau5485>.
- [3] Centers for Disease Control and Prevention (2017) Influenza (Flu), Centers for Disease Control and Prevention.. <https://www.cdc.gov/flu/avianflu/monitoring-bird-flu.html> (accessed September 4, 2020).
- [4] Z. Beau Reneer, T.M. Ross, H2 influenza viruses: Designing vaccines against future H2

- pandemics, *Biochem. Soc. Trans.* 47 (2019) 251–264. <https://doi.org/10.1042/BST20180602>.
- [5] R.J. Garten, C.T. Davis, C.A. Russell, B. Shu, S. Lindstrom, A. Balish, W.M. Sessions, X. Xu, E. Skepner, V. Deyde, M. Okomo-Adhiambo, L. Gubareva, J. Barnes, C.B. Smith, S.L. Emery, M.J. Hillman, P. Rivaller, J. Smagala, M. De Graaf, D.F. Burke, R.A.M. Fouchier, C. Pappas, C.M. Alpuche-Aranda, H. López-Gatell, H. Olivera, I. López, C.A. Myers, D. Faix, P.J. Blair, C. Yu, K.M. Keene, P.D. Dotson, D. Boxrud, A.R. Sambol, S.H. Abid, K. St. George, T. Bannerman, A.L. Moore, D.J. Stringer, P. Blevins, G.J. Demmler-Harrison, M. Ginsberg, P. Kriner, S. Waterman, S. Smole, H.F. Guevara, E.A. Belongia, P.A. Clark, S.T. Beatrice, R. Donis, J. Katz, L. Finelli, C.B. Bridges, M. Shaw, D.B. Jernigan, T.M. Uyeki, D.J. Smith, A.I. Klimov, N.J. Cox, Antigenic and genetic characteristics of swine-origin 2009 A(H1N1) influenza viruses circulating in humans, *Science* (80-.). 325 (2009) 197–201. <https://doi.org/10.1126/science.1176225>.
- [6] W.R. Dowdle, Influenza A virus recycling revisited., *Bull World Heal. Organ* . 77 (1999) 820–828.
- [7] Y. Lu, S. Landreth, A. Gaba, M. Hlasny, G. Liu, Y. Huang, Y. Zhou, In vivo characterization of avian influenza a (H5N1) and (H7N9) viruses isolated from canadian travelers, *Viruses*. 11 (2019) 193–205. <https://doi.org/10.3390/v11020193>.
- [8] M.G. Ison, Antiviral Treatments, *Clin. Chest Med.* 38 (2017) 139–153. <https://doi.org/10.1016/j.ccm.2016.11.008>.
- [9] V. Peltola, E.A. Govorkova, E.A. Hernandez-Vargas, S. Esposito, N. Principi, B. Camilloni, A. Alunno, I. Polinori, A. Argentiero, Drugs for Influenza Treatment: Is There Significant News?, *Front. Med.* 1 (2019) 109–115. <https://doi.org/10.3389/fmed.2019.00109>.
- [10] M. Toots, R.K. Plemper, Next-generation direct-acting influenza therapeutics, *Transl. Res.* 220 (2020) 33–42. <https://doi.org/10.1016/j.trsl.2020.01.005>.
- [11] F.G. Hayden, N. Shindo, Influenza virus polymerase inhibitors in clinical development, *Curr. Opin. Infect. Dis.* 32 (2019) 176–186. <https://doi.org/10.1097/QCO.0000000000000532>.

- [12] E.J. Mifsud, F.G. Hayden, A.C. Hurt, Antivirals targeting the polymerase complex of influenza viruses., *Antiviral Res.* 169 (2019) 104545–104554.
<https://doi.org/10.1016/j.antiviral.2019.104545>.
- [13] Y. Furuta, B.B. Gowen, K. Takahashi, K. Shiraki, D.F. Smee, D.L. Barnard, Favipiravir (T-705), a novel viral RNA polymerase inhibitor, *Antiviral Res.* 100 (2013) 446–454.
<https://doi.org/10.1016/j.antiviral.2013.09.015>.
- [14] T. Noshi, M. Kitano, K. Taniguchi, A. Yamamoto, S. Omoto, K. Baba, T. Hashimoto, K. Ishida, Y. Kushima, K. Hattori, M. Kawai, R. Yoshida, M. Kobayashi, T. Yoshinaga, A. Sato, M. Okamoto, Y. Sakoda, H. Kida, T. Shishido, A. Naito, In vitro characterization of baloxavir acid, a first-in-class cap-dependent endonuclease inhibitor of the influenza virus polymerase PA subunit, *Antiviral Res.* 160 (2018) 109–117.
<https://doi.org/10.1016/j.antiviral.2018.10.008>.
- [15] M.P. Clark, M.W. Ledebroer, I. Davies, R.A. Byrn, S.M. Jones, E. Perola, A. Tsai, M. Jacobs, K. Nti-Addae, U.K. Bandarage, M.J. Boyd, R.S. Bethiel, J.J. Court, H. Deng, J.P. Duffy, W.A. Dorsch, L.J. Farmer, H. Gao, W. Gu, K. Jackson, D.H. Jacobs, J.M. Kennedy, B. Ledford, J. Liang, F. Maltais, M. Murcko, T. Wang, M.W. Wannamaker, H.B. Bennett, J.R. Leeman, C. McNeil, W.P. Taylor, C. Memmott, M. Jiang, R. Rijnbrand, C. Bral, U. Germann, A. Nezami, Y. Zhang, F.G. Salituro, Y.L. Bennani, P.S. Charifson, Discovery of a novel, first-in-class, orally bioavailable azaindole inhibitor (VX-787) of influenza PB2., *J. Med. Chem.* 57 (2014) 6668–78. <https://doi.org/10.1021/jm5007275>.
- [16] A. Loregian, B. Mercorelli, G. Nannetti, C. Compagnin, G. Palù, Antiviral strategies against influenza virus: towards new therapeutic approaches., *Cell. Mol. Life Sci.* 71 (2014) 3659–83. <https://doi.org/10.1007/s00018-014-1615-2>.
- [17] J. Zhang, Y. Hu, R. Musharrafieh, H. Yin, J. Wang, Focusing on the Influenza Virus Polymerase Complex: Recent Progress in Drug Discovery and Assay Development, *Curr. Med. Chem.* 26 (2018) 2243–2263. <https://doi.org/10.2174/0929867325666180706112940>.

- [18] I. Giacchello, F. Musumeci, I. D'Agostino, C. Greco, G. Grossi, S. Schenone, Insights into RNA-dependent RNA Polymerase Inhibitors as Anti-influenza Virus Agents., *Curr. Med. Chem.* 27 (2020) 1. <https://doi.org/10.2174/0929867327666200114115632>.
- [19] J.M. Wandzik, T. Kouba, S. Cusack, Structure and Function of Influenza Polymerase, *Cold Spring Harb Perspect Med.* 9 (2020) 38372–38391. <https://doi.org/10.1101/cshperspect.a038372>.
- [20] E. Fodor, A.J.W. te Velthuis, Structure and Function of the Influenza Virus Transcription and Replication Machinery, *Cold Spring Harb. Perspect. Med.* 9 (2019) 38398–38413. <https://doi.org/10.1101/cshperspect.a038398>.
- [21] X. He, J. Zhou, M. Bartlam, R. Zhang, J. Ma, Z. Lou, X. Li, J. Li, A. Joachimiak, Z. Zeng, R. Ge, Z. Rao, Y. Liu, Crystal structure of the polymerase PAC–PB1N complex from an avian influenza H5N1 virus, *Nature.* 454 (2008) 1123–1126. <https://doi.org/10.1038/nature07120>.
- [22] E. Obayashi, H. Yoshida, F. Kawai, N. Shibayama, A. Kawaguchi, K. Nagata, J.R.H. Tame, S.-Y. Park, The structural basis for an essential subunit interaction in influenza virus RNA polymerase., *Nature.* 454 (2008) 1127–31. <https://doi.org/10.1038/nature07225>.
- [23] G. Palù, A. Loregian, Inhibition of herpesvirus and influenza virus replication by blocking polymerase subunit interactions, *Antiviral Res.* 99 (2013) 318–327. <https://doi.org/10.1016/j.antiviral.2013.05.014>.
- [24] S. Massari, L. Goracci, J. Desantis, O. Tabarrini, Polymerase Acidic Protein–Basic Protein 1 (PA–PB1) Protein–Protein Interaction as a Target for Next-Generation Anti-influenza Therapeutics, *J. Med. Chem.* 59 (2016) 7699–7718. <https://doi.org/10.1021/acs.jmedchem.5b01474>.
- [25] S. Massari, J. Desantis, M.G. Nizi, V. Cecchetti, O. Tabarrini, Inhibition of Influenza Virus Polymerase by Interfering with Its Protein-Protein Interactions, *ACS Infect. Dis.* (2020). <https://doi.org/https://dx.doi.org/10.1021/acsinfecdis.0c00552>.
- [26] G. Muratore, B. Mercorelli, L. Goracci, G. Cruciani, P. Digard, G. Palù, A. Loregian, Human

cytomegalovirus inhibitor AL18 also possesses activity against influenza A and B viruses, *Antimicrob. Agents Chemother.* 56 (2012) 6009–6013. <https://doi.org/10.1128/AAC.01219-12>.

- [27] G. Muratore, L. Goracci, B. Mercorelli, Á. Foeglein, P. Digard, G. Cruciani, G. Palù, A. Loregian, Small molecule inhibitors of influenza A and B viruses that act by disrupting subunit interactions of the viral polymerase, *Proc. Natl. Acad. Sci. U. S. A.* 109 (2012) 6247–6252. <https://doi.org/10.1073/pnas.1119817109>.
- [28] I.M.L. Trist, G. Nannetti, C. Tintori, A.L. Fallacara, D. Deodato, B. Mercorelli, G. Palù, M. Wijtmans, T. Gospodova, E. Edink, M. Verheij, I. De Esch, L. Viteva, A. Loregian, M. Botta, 4,6-Diphenylpyridines as Promising Novel Anti-Influenza Agents Targeting the PA-PB1 Protein-Protein Interaction: Structure-Activity Relationships Exploration with the Aid of Molecular Modeling, *J. Med. Chem.* 59 (2016) 2688–2703. <https://doi.org/10.1021/acs.jmedchem.5b01935>.
- [29] S. Massari, G. Nannetti, L. Goracci, L. Sancineto, G. Muratore, S. Sabatini, G. Manfroni, B. Mercorelli, V. Cecchetti, M. Facchini, G. Palù, G. Cruciani, A. Loregian, O. Tabarrini, Structural investigation of cycloheptathiophene-3-carboxamide derivatives targeting influenza virus polymerase assembly, *J. Med. Chem.* 56 (2013) 10118–10131. <https://doi.org/10.1021/jm401560v>.
- [30] J. Desantis, G. Nannetti, S. Massari, M.L. Barreca, G. Manfroni, V. Cecchetti, G. Palù, L. Goracci, A. Loregian, O. Tabarrini, Exploring the cycloheptathiophene-3-carboxamide scaffold to disrupt the interactions of the influenza polymerase subunits and obtain potent anti-influenza activity, *Eur. J. Med. Chem.* 138 (2017) 128–139. <https://doi.org/10.1016/j.ejmech.2017.06.015>.
- [31] G. Nannetti, S. Massari, B. Mercorelli, C. Bertagnin, J. Desantis, G. Palù, O. Tabarrini, A. Loregian, Potent and broad-spectrum cycloheptathiophene-3-carboxamide compounds that target the PA-PB1 interaction of influenza virus RNA polymerase and possess a high barrier

to drug resistance, *Antiviral Res.* 165 (2019) 55–64.

<https://doi.org/10.1016/j.antiviral.2019.03.003>.

- [32] S. Massari, G. Nannetti, J. Desantis, G. Muratore, S. Sabatini, G. Manfroni, B. Mercorelli, V. Cecchetti, G. Palù, G. Cruciani, A. Loregian, L. Goracci, O. Tabarrini, A Broad anti-influenza hybrid small molecule that potently disrupts the interaction of polymerase acidic protein-basic protein 1 (PA-PB1) subunits, *J. Med. Chem.* 58 (2015) 3830–3842.
<https://doi.org/10.1021/acs.jmedchem.5b00012>.
- [33] S. Lepri, G. Nannetti, G. Muratore, G. Cruciani, R. Ruzziconi, B. Mercorelli, G. Palù, A. Loregian, L. Goracci, Optimization of Small-Molecule Inhibitors of Influenza Virus Polymerase: From Thiophene-3-Carboxamide to Polyamido Scaffolds, *J. Med. Chem.* 57 (2014) 4337–4350. <https://doi.org/10.1021/jm500300r>.
- [34] I. D'Agostino, I. Giacchello, G. Nannetti, A.L. Fallacara, D. Deodato, F. Musumeci, G. Grossi, G. Palù, Y. Cau, I.M. Trist, A. Loregian, S. Schenone, M. Botta, Synthesis and biological evaluation of a library of hybrid derivatives as inhibitors of influenza virus PA-PB1 interaction, *Eur. J. Med. Chem.* 157 (2018) 743–758.
<https://doi.org/10.1016/j.ejmech.2018.08.032>.
- [35] H. Liu, X. Yao, Molecular basis of the interaction for an essential subunit PA-PB1 in influenza virus RNA polymerase: insights from molecular dynamics simulation and free energy calculation., *Mol. Pharm.* 7 (2010) 75–85. <https://doi.org/10.1021/mp900131p>.
- [36] V.M. Chernyshev, A. V. Chernysheva, V.A. Taranushich, Synthesis of esters and amides of 5-amino-1,2,4-triazole-3-carboxylic and 5-amino-1,2,4-triazol-3-ylacetic acids, *Russ. J. Appl. Chem.* 79 (2006) 783–786. <https://doi.org/10.1134/S1070427206050168>.
- [37] S. Massari, J. Desantis, G. Nannetti, S. Sabatini, S. Tortorella, L. Goracci, V. Cecchetti, A. Loregian, O. Tabarrini, Efficient and regioselective one-step synthesis of 7-aryl-5-methyl- and 5-aryl-7-methyl-2-amino-[1,2,4]triazolo[1,5-a]pyrimidine derivatives, *Org. Biomol. Chem.* 15 (2017) 7944–7955. <https://doi.org/10.1039/C7OB02085F>.

- [38] E. Sopbué Fondjo, D. Döpp, G. Henkel, Reactions of some anellated 2-aminothiophenes with electron poor acetylenes, *Tetrahedron*. 62 (2006) 7121–7131.
<https://doi.org/10.1016/j.tet.2006.04.037>.
- [39] T. Masaoka, S. Chung, P. Caboni, J.W. Rausch, J.A. Wilson, H. Taskent-Sezgin, J.A. Beutler, G. Tocco, S.F.J. Le Grice, Exploiting drug-resistant enzymes as tools to identify thienopyrimidinone inhibitors of human immunodeficiency virus reverse transcriptase-associated ribonuclease H, *J. Med. Chem.* 56 (2013) 5436–5445.
<https://doi.org/10.1021/jm400405z>.
- [40] K.P. Ravindranathan, V. Mandiyan, A.R. Ekkati, J.H. Bae, J. Schlessinger, W.L. Jorgensen, Discovery of novel fibroblast growth factor receptor 1 kinase inhibitors by structure-based virtual screening., *J. Med. Chem.* 53 (2010) 1662–72. <https://doi.org/10.1021/jm901386e>.
- [41] V. Kogan, Preparation of pyrido[3,4-b]indoles and pyrimido[4,5-b]benzo[d]thiophen-4-ones as serotonergic and dopaminergic agents, WO2008/117269 A2, 2008.
- [42] T. Morwick, A. Berry, J. Brickwood, M. Cardozo, K. Catron, M. DeTuri, J. Emeigh, C. Homon, M. Hrapchak, S. Jacober, S. Jakes, P. Kaplita, T.A. Kelly, J. Ksiazek, M. Liuzzi, R. Magolda, C. Mao, D. Marshall, D. McNeil, A. Prokopowicz, C. Sarko, E. Scouten, C. Sledziona, S. Sun, J. Watrous, J.P. Wu, C.L. Cywin, Evolution of the Thienopyridine Class of Inhibitors of I κ B Kinase- β : Part I: Hit-to-Lead Strategies, *J. Med. Chem.* 49 (2006) 2898–2908. <https://doi.org/10.1021/jm0510979>.
- [43] K. Usui, K. Tanoue, K. Yamamoto, T. Shimizu, H. Suemune, Synthesis of substituted azulenes via Pt(II)-Catalyzed ring-expanding cycloisomerization, *Org. Lett.* 16 (2014) 4662–4665. <https://doi.org/10.1021/ol502270q>.
- [44] Y. Güneş, M.F. Polat, E. Sahin, F.F. Fleming, R. Altundas, Enantioselective synthesis of cyclic, quaternary oxonitriles, *J. Org. Chem.* 75 (2010) 7092–7098.
<https://doi.org/10.1021/jo1011202>.
- [45] S. Massari, A. Corona, S. Distinto, J. Desantis, A. Caredda, S. Sabatini, G. Manfroni, T.

- Felicetti, V. Cecchetti, C. Pannecouque, E. Maccioni, E. Tramontano, O. Tabarrini, From cycloheptathiophene-3-carboxamide to oxazinone-based derivatives as allosteric HIV-1 ribonuclease H inhibitors, *J. Enzyme Inhib. Med. Chem.* 34 (2019) 55–74.
<https://doi.org/10.1080/14756366.2018.1523901>.
- [46] R. Romagnoli, P.G. Baraldi, M. Kimatrai Salvador, D. Preti, M. Aghazadeh Tabrizi, M. Bassetto, A. Brancale, E. Hamel, I. Castagliuolo, R. Bortolozzi, G. Basso, G. Viola, Synthesis and biological evaluation of 2-(alkoxycarbonyl)-3-anilinobenzo[b]thiophenes and thieno[2,3-b]pyridines as new potent anticancer agents, *J. Med. Chem.* 56 (2013) 2606–18.
<https://doi.org/10.1021/jm400043d>.
- [47] P. Leonczak, L.-J. Gao, A.T. Ramadori, E. Lescrinier, J. Rozenski, S. De Jonghe, P. Herdewijn, Synthesis and structure-activity relationship studies of 2-(1,3,4-oxadiazole-2(3H)-thione)-3-amino-5-arylthieno[2,3-b]pyridines as inhibitors of DRAK2., *ChemMedChem*. 9 (2014) 2587–601. <https://doi.org/10.1002/cmdc.201402234>.
- [48] T.D. Graneto, Matthew; Hanau, Cathleen E.; Perry, Heteroaromatic carboxamide derivatives, particularly 3-aminothiophene-2-carboxamides, useful as protein kinase inhibitors, for the treatment of cancer, inflammation, and inflammation-related disorders, WO03037886 (A2), 2003.
- [49] L.H. Klemm, J. Wang, L. Hawkins, Synthesis of 3-amino-2-carbamoylthiophene and its reaction with cycloalkanones to form imines, *J. Heterocycl. Chem.* 32 (1995) 1039–1041.
<https://doi.org/10.1002/jhet.5570320361>.
- [50] B.E. Sleebbs, A. Levit, I.P. Street, H. Falk, T. Hammonds, A.C. Wong, M.D. Charles, M.F. Olson, J.B. Baell, Identification of 3-aminothieno[2,3-b]pyridine-2-carboxamides and 4-aminobenzothieno[3,2-d]pyrimidines as LIMK1 inhibitors, *Medchemcomm.* 2 (2011) 977–981. <https://doi.org/10.1039/c1md00137j>.
- [51] N.Y. Gorobets, B.H. Yousefi, F. Belaj, C.O.O. Kappe, Rapid microwave-assisted solution phase synthesis of substituted 2-pyridone libraries, *Tetrahedron.* 60 (2004) 8633–8644.

<https://doi.org/10.1016/j.tet.2004.05.100>.

- [52] F. Perrissin, M.; Luu, D.C.; Narcisse, G.; Bakri-Logeais, F.; Huguet, 4,5,6,7-Tetrahydrobenzo[b]- and 5,6,7,8-tetrahydro-4H-cyclohepta[b]thiophenes., *Eur. J. Med. Chem.* 15 (1980) 413–418.
- [53] Compounds 14 and 23 were previously reported by us in a paper (reference 14) focused on the development of suitable procedures for the synthesis of the [1,2,4]-triazolo[1,5-a]pyrimidine nucleus.
- [54] C. Aldrich, C. Bertozzi, G.I. Georg, L. Kiessling, C. Lindsley, D. Liotta, K.M. Merz, A. Schepartz, S. Wang, The Ecstasy and Agony of Assay Interference Compounds, *ACS Cent. Sci.* 3 (2017) 143–147. <https://doi.org/10.1021/acscentsci.7b00069>.
- [55] T. Sterling, J.J. Irwin, ZINC 15 – Ligand Discovery for Everyone, *J. Chem. Inf. Model.* 55 (2015) 2324–2337. <https://doi.org/10.1021/acs.jcim.5b00559>.
- [56] A. Daina, O. Michielin, V. Zoete, SwissADME: A free web tool to evaluate pharmacokinetics, drug-likeness and medicinal chemistry friendliness of small molecules, *Sci. Rep.* 7 (2017) 1–13. <https://doi.org/10.1038/srep42717>.
- [57] C.A.S. Bergström, W.N. Charman, C.J.H. Porter, Computational prediction of formulation strategies for beyond-rule-of-5 compounds, *Adv. Drug Deliv. Rev.* 101 (2016) 6–21. <https://doi.org/10.1016/j.addr.2016.02.005>.
- [58] C.M. Wassvik, A.G. Holmén, R. Draheim, P. Artursson, C.A.S. Bergström, Molecular characteristics for solid-state limited solubility, *J. Med. Chem.* 51 (2008) 3035–3039. <https://doi.org/10.1021/jm701587d>.
- [59] C. Janiak, A critical account on π - π stacking in metal complexes with aromatic nitrogen-containing ligands †, *J. Chem. Soc. Dalt. Trans.* (2000) 3885–3896. <https://doi.org/10.1039/b003010o>.
- [60] B. Bonn, C. Leandersson, F. Fontaine, I. Zamora, Enhanced metabolite identification with MS^E and a semi-automated software for structural elucidation, *Rapid Commun. Mass*

- Spectrom. 24 (2010) 3127–3138. <https://doi.org/10.1002/rcm.4753>.
- [61] I. Zamora, F. Fontaine, B. Serra, G. Plasencia, High-throughput, computer assisted, specific MetID. A revolution for drug discovery, *Drug Discov. Today Technol.* 10 (2013) e199–e205. <https://doi.org/10.1016/j.ddtec.2012.10.015>.
- [62] A. Brink, F. Fontaine, M. Marschmann, B. Steinhuber, E.N. Cece, I. Zamora, A. Pähler, Post-acquisition analysis of untargeted accurate mass quadrupole time-of-flight MS^E data for multiple collision-induced neutral losses and fragment ions of glutathione conjugates, *Rapid Commun. Mass Spectrom.* 28 (2014) 2695–2703. <https://doi.org/10.1002/rcm.7062>.
- [63] T. Radchenko, F. Fontaine, L. Moretoni, I. Zamora, WebMetabase: Cleavage sites analysis tool for natural and unnatural substrates from diverse data source, *Bioinformatics.* 35 (2019) 650–655. <https://doi.org/10.1093/bioinformatics/bty667>.
- [64] G. Cruciani, E. Carosati, B. De Boeck, K. Ethirajulu, C. Mackie, T. Howe, R. Vianello, MetaSite: Understanding metabolism in human cytochromes from the perspective of the chemist, *J. Med. Chem.* 48 (2005) 6970–6979. <https://doi.org/10.1021/jm050529c>.
- [65] M. Baroni, G. Cruciani, S. Sciabola, F. Perruccio, J.S. Mason, A common reference framework for analyzing/comparing proteins and ligands. Fingerprints for Ligands and Proteins (FLAP): Theory and application, *J. Chem. Inf. Model.* 47 (2007) 279–294. <https://doi.org/10.1021/ci600253e>.
- [66] T. Masaoka, S. Chung, P. Caboni, J.W. Rausch, J.A. Wilson, H. Taskent-Sezgin, J.A. Beutler, G. Tocco, S.F.J. Le Grice, Exploiting drug-resistant enzymes as tools to identify thienopyrimidinone inhibitors of human immunodeficiency virus reverse transcriptase-associated ribonuclease H., *J. Med. Chem.* 56 (2013) 5436–45. <https://doi.org/10.1021/jm400405z>.
- [67] G. Cruciani, F. Milletti, L. Storchi, G. Sforza, L. Goracci, *In silico* pK_a Prediction and ADME Profiling, *Chem. Biodivers.* 6 (2009) 1812–1821. <https://doi.org/10.1002/cbdv.200900153>.

- [68] S. Fawell, J. Seery, Y. Daikh, C. Moore, L.L. Chen, B. Pepinsky, J. Barsoum, Tat-mediated delivery of heterologous proteins into cells, *Proc. Natl. Acad. Sci. U. S. A.* 91 (1994) 664–668.
- [69] A. Loregian, B.A. Appleton, J.M. Hogle, D.M. Coen, Residues of Human Cytomegalovirus DNA Polymerase Catalytic Subunit UL54 That Are Necessary and Sufficient for Interaction with the Accessory Protein UL44, *J. Virol.* 78 (2004) 158–167.
<https://doi.org/10.1128/jvi.78.1.158-167.2004>.
- [70] A. Loregian, D.M. Coen, Selective anti-cytomegalovirus compounds discovered by screening for inhibitors of subunit interactions of the viral polymerase, *Chem. Biol.* 13 (2006) 191–200.
<https://doi.org/10.1016/j.chembiol.2005.12.002>.
- [71] K.A. Dehring, H.L. Workman, K.D. Miller, A. Mandagere, S.K. Poole, Automated robotic liquid handling/laser-based nephelometry system for high throughput measurement of kinetic aqueous solubility, *J. Pharm. Biomed. Anal.* 36 (2004) 447–456.
<https://doi.org/10.1016/j.jpba.2004.07.022>.

Highlights

- New hybrid compounds based on the 1,2,4-triazolo[1,5-*a*]pyrimidine-2-carboxamide nucleus were identified showing anti-flu activity by disrupting polymerase PA-PB1 interaction.
- The cycloheptathiophene can be replaced by a simple phenyl ring, with advantages in the synthetic processes as well as in the solubility of the compound.
- Molecular docking study has rationalized the binding mode of the compounds within the PA_C.

Declaration of interests

The authors declare that they have no known competing financial interests or personal relationships that could have appeared to influence the work reported in this paper.

The authors declare the following financial interests/personal relationships which may be considered as potential competing interests:

Journal Pre-proof